Dendrochronologia 71 (2022) 125913

Contents lists available at ScienceDirect

Dendrochronologia

journal homepage: www.elsevier.com/locate/dendro

Climate-growth relations of congeneric tree species vary across a tropical vegetation gradient in Brazil

José Roberto V. Aragão [a,*], Pieter A. Zuidema [b], Peter Groenendijk [a]

[a] Department of Plant Biology, Institute of Biology, University of Campinas (UNICAMP), P.O. Box: 6109, 13083-970 Campinas, SP, Brazil
[b] Forest Ecology & Forest Management Group, Wageningen University, Wageningen, The Netherlands

ARTICLE INFO

Keywords:
Tree-rings
Seasonally dry tropical forests
Drought effects
Climate change
Environmental gradient

ABSTRACT

Seasonally dry tropical forests are an important global climatic regulator, a main driver of the global carbon sink dynamics and are predicted to suffer future reductions in their productivity due to climate change. Yet, little is known about how interannual climate variability affects tree growth and how climate-growth responses vary across rainfall gradients in these forests. Here we evaluate changes in climate sensitivity of tree growth along an environmental gradient of seasonally dry tropical vegetation types (evergreen forest – savannah – dry forest) in Northeastern Brazil, using congeneric species of two common neotropical genera: *Aspidosperma* and *Handroanthus*. We built tree-ring width chronologies for each species × forest type combinations and explored how growth variability correlated with local (precipitation, temperature) and global (the El Niño Southern Oscillation - ENSO) climatic factors. We also assessed how growth sensitivity to climate and the presence of growth deviations varied along the gradient. Precipitation stimulates tree growth and was the main growth-influencing factor across vegetation types. Trees in the dry forest site showed highest growth sensitivity to interannual variation in precipitation. Temperature and ENSO phenomena correlated negatively with growth and sensitivity to both climatic factors were similar across sites. Negative growth deviations were present and found mostly in the dry-forest species. Our results reveal a dominant effect of precipitation on tree growth in seasonally dry tropical forests and suggest that along the gradient, dry forests are the most sensitivity to drought. These forests may therefore be the most vulnerable to the deleterious effects of future climatic changes. These results highlight the importance of understanding the climatic sensitivity of different tropical forests. This understanding is key to predict the carbon dynamics in tropical regions, and sensitivity differences should be considered when prioritizing conservation measures of seasonally dry topical forests.

1. Introduction

Tropical forests are among the main climate regulators of the planet (Chazdon et al., 2016; Le Quéré et al., 2018). Over the past 20 years, they have stored three times more atmospheric CO_2 (3.59 PgC yr - 1) than other forests (Xu et al., 2021) and sequestered a quarter of all carbon in terrestrial ecosystems (Le Quéré et al., 2018). Seasonally dry tropical forests are particularly important as a climatic regulator (Piao et al., 2020b), acting as a carbon sink in seasonal productivity cycles (Linscheid et al., 2020; Piao et al., 2020a, 2020b; Sitch et al., 2003) that are modulated by interannual variation (IAV, i.e., the variation between years) in temperature and precipitation (Linscheid et al., 2020; Piao et al., 2020b). The strong climatic variability experienced by seasonally dry tropical forest regions (Ahlstrom et al., 2015) and their position within atmospheric systems, induce regional oscillations in rainfall that drive the high IAV in productivity of these forests (Asmerom et al., 2020; Ciemer et al., 2019). Despite the importance of these forest and the strong climatic variation they experience, empirical information on the magnitude and drivers of climate-driven variability in the productivity of seasonally dry forests is scarce (Frank et al., 2015; Pennington et al., 2018).

Climate change projections predict alterations of the IAV of tropical dry forest productivity, possibly resulting in reduced forest cover and biomass (Chen et al., 2019; Humphrey, 2021; Piao et al., 2020b). These changes may cause reductions in the growing season length of trees (Piao et al., 2020b; Poulter et al., 2014) and, consequently, a drop in primary productivity (GPP) (Ahlström et al., 2015; Frank et al., 2015). Such GPP reductions are enhanced during global climatic events such as

* Corresponding author.
E-mail address: craniusru@gmail.com (J.R.V. Aragão).

https://doi.org/10.1016/j.dendro.2021.125913
Received 27 August 2021; Received in revised form 13 November 2021; Accepted 18 November 2021
Available online 26 November 2021

the positive phase of the El Niño Southern Oscillation, which tends to increase water deficit in seasonally dry forests (Bastos et al., 2018; Zhang and Jia, 2020). Under climate-change scenarios, these global climatic events are expected to increase in frequency (Stan and Sanchez-Azofeifa, 2019), and thus to reduce the growth and resilience of tree species in seasonal tropical forests (Gao et al., 2018). Understanding the sensitivity of different seasonally dry tropical forests to climatic variability, and how this sensitivity is modulated by extreme climatic events is thus crucial to understand the responses of these forests to future climatic changes (Ciemer et al., 2019; Zhang and Jia, 2020; Zhao et al., 2018). Yet, we have little empirical data on the climate sensitivity of productivity of these forests and how this sensitivity varies across vegetation types and climatic gradients (Ciemer et al., 2019; Zhang and Jia, 2020; Zhao et al., 2018).

An important and structural component of seasonally dry forests primary productivity is woody growth, which is dominated by tree stem growth (Bloom et al., 2020). Studies on tree stem growth can thus be used to evaluate responses of seasonally dry tropical forests to climate variability (Brodribb et al., 2020; Gao et al., 2018; Kannenberg et al., 2020; Wang et al., 2016). Tree-ring analyses can be used to assess stem growth responses to climate variability as the variation in ring width between years stores information on how interannual climatic variability affects tree growth over large spatio-temporal scales (Zuidema et al., 2013; Zuidema and Frank, 2015). Although increasingly being applied in tropical regions (Babst et al., 2018), tropical forests are still strongly underrepresented in these types of studies.

When applied along environmental gradients, tree-ring studies can help to understand climatic responses of different forest types (Godoy-Veiga et al., 2021; López et al., 2019), to assess which local environmental characteristics modulate tree growth and its IAV (Anning et al., 2013; López et al., 2019) and understand their temporal relationship with climate (Camarero et al., 2013; Ciemer et al., 2019; Meko et al., 2011). For instance, in seasonally dry tropical forest, climate sensitivity of tree growth was found to increase with increasing water deficit (Godoy-Veiga et al., 2021; López et al., 2019). One complicating factor of such studies in tropical forests is the high diversity of tree species and large species turnover along environmental gradients (Banda-R et al., 2016). To accommodate this problem, studies along environmental gradients have also been performed using congeneric species (Locosselli et al., 2017). The genetic proximity, and similarities in functional traits and wood characteristics reduce species differences (Fernández Otárola et al., 2016) as well as phylogenetic distance (Felsenstein, 1985).

Here we present an analysis of the shifts in climate responses of tree growth along an environmental gradient of seasonally dry tropical vegetation types (evergreen forest – savannah – dry forest) using congeneric species of two common neotropical genera: *Aspidosperma* and *Handroanthus*. These two genera were selected for their wide distribution in tropical seasonal forests, ecological importance (Fernandes et al., 2020; Queiroz et al., 2017), and potential for building chronologies (Andrade et al., 2019; Aragão et al., 2019; Espinosa et al., 2018; López and Villalba, 2020). We assessed growth sensitivity by exploring standard chronology statistics of growth synchronicity, by evaluating the strength of the climatic effect on growth variability (slopes and R^2 of climate-growth regressions) and by looking at differences in the amount of growth deviations (pointer years) along this gradient. We addressed the following hypotheses: 1) At all sites, annual growth variability within species is synchronized and driven by annual variability in water deficit; 2) for all study species across the gradient, growth will correlate with monthly sea surface temperatures and will be negatively affected by monthly El Niño index values encompassing the period around the growing season; 3) growth responses of the two genera converge along the gradient, with growth being increasingly more sensitive to climate, that is, showing stronger climate-growth relationships (slopes and R^2 of the regressions) as average water deficit increases from evergreen forest to dry forest; and 4) within genera, dry forests species will show more growth reductions (e.g., Gao et al., 2018) due to their more sensitive response to climate variation and water availability.

This is one of the first studies using tree-ring analyses to assess how climate-growth relationships change across gradients of forests types in tropical arid regions (Brienen et al., 2016; Pompa-García and Camarero, 2020; Schöngart et al., 2017). As a first step in our study, we confirmed the dendrochronological potential of our species by assessing the anatomical structures delimiting their tree rings. The annual nature of tree-ring formation was confirmed by the strong growth synchronicity between individuals and strong climate-growth correlations. Growth variability was correlated with local meteorological data (precipitation and temperature) and large-scale climatic variables (e.g., global sea surface temperatures, El Niño indices). Finally, we compared how growth sensitivity and growth deviations change in our populations along the gradient (Gao et al., 2018).

2. Material and methods

2.1. Study area

Trees were sampled in three sites located in protected areas of seasonally dry topical forests in the states of Ceará and Piauí, in Northeastern Brazil (Fig. 1). The three localities fall within the larger seasonally neotropical dry forest biomes known as *Caatinga* and *Cerrado*, but comprise a gradient of vegetation types presenting evergreen forest, savannah and dry forests (Fernandes et al., 2020; Queiroz et al., 2017; Silveira et al., 2020). This gradient in vegetation types is reflected by the environmental conditions of each site: the evergreen forest and savannah sites have similar total annual precipitation levels, but differ in precipitation seasonality, mean annual temperature and the presence of aquifers (at the savanna), while the dry-forest site has the lowest total annual precipitation and presents high temperatures.

Our evergreen-forest site was located at the Ubajara National Park (Fig. 1) in the northwest of Ceará state (3°54'34"S and 40°59'24"W). This site is characterized as an evergreen forest (Silveira et al., 2020) with strong taxonomic Amazonian influence (Moro et al., 2015). It is located on a plateau on the sedimentary basins of the Ibiapaba complex (Moro et al., 2016; Silva et al., 2017; Silveira et al., 2020), with predominance of Ferralsols (FAO, 2014; Santos et al., 2011, 2018). Climate of the evergreen-forest site falls in the transient category between tropical savannah (Aw) and semi-arid (BSh). Precipitation at this site is under strong influence of the Intertropical Convergence Zone (ITCZ; Andrade et al., 2017), falling mostly during the austral summer (December till May), with a dry season in winter (Köppen, 1948). Mean temperatures range between 22° and 24 °C and average annual precipitation amounts 1.460 mm, concentrated mainly between the months of February-March-April (Araújo et al., 1999). Due to the topography and prevailing wind direction, this site has a strong effect of orographic precipitation (Silveira et al., 2020).

Our savannah site was in the Sete Cidades National Park (Fig. 1) in northern Piauí state (04°02'08"S and 41°40"45"W). This site is characterized as a neotropical savannah vegetation (*Cerrado*) (Oliveira and Marquis, 2002). Soils are sandy, sedimentary with a predominance of Entisols (Santos et al., 2011, 2018; Soil Survey Staff, 2014), with occurrence of underground aquifers (Andrade et al., 2017; Matos and Felfili, 2010). Climate of the savannah site also falls in the transient category between tropical savannah (Aw) and semi-arid (BSh). This site is also is under strong influence of the ITCZ (Andrade et al., 2017), with precipitation concentrated during the austral summer and a strong dry season in winter (Köppen, 1948). Mean temperatures range between 25° and 28 °C and annual precipitation averages 1.350 mm with a peak between April-March (Andrade et al., 2017; Matos and Felfili, 2010).

Our dry-forest site was located at the Aiuaba Ecological Station (Estação Ecológica de Aiuaba; Fig. 1), in southwest Ceará state (06°36'00"S and 40°10'00"O). This site is characterized as a typical neotropical dry-forest vegetation (*Caatinga*). Its geological formations

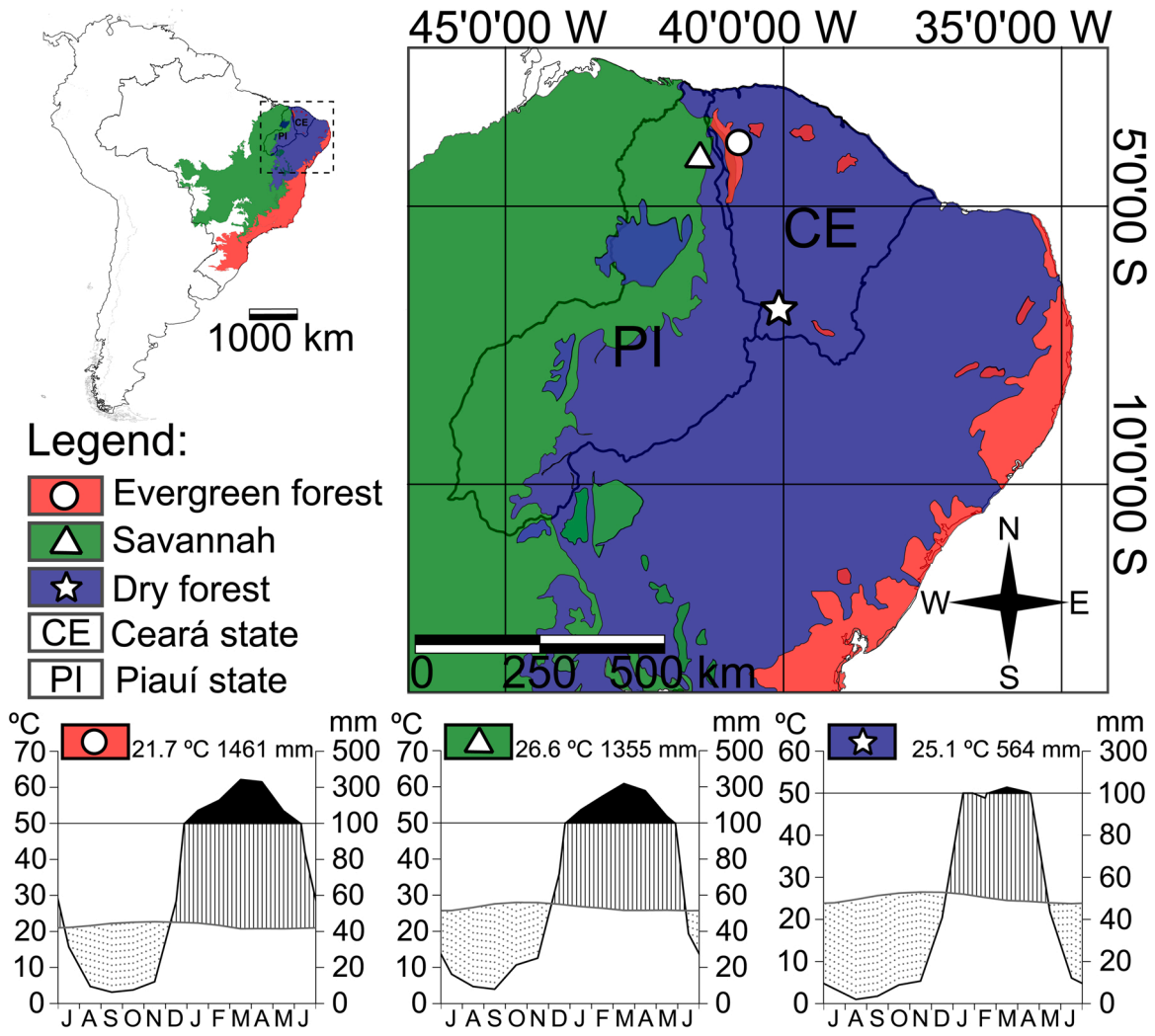

Fig. 1. Locations of the three study sites along a neotropical seasonal vegetation gradient (classified cf. Olson et al., 2001) in the states of Ceará (CE) and Piauí(PI) in Northeastern Brazil: evergreen forest (red-circle) in the Ubajara National Park, neotropical savannah (green-triangle) in the Sete Cidades National Park and tropical dry forest (blue-star) in the Aiuaba Ecological Station. Climate diagrams for the period 1978–2018 (cf. Walter and Lieth, 1960) for each site are also provided: gray lines show mean monthly temperatures, black lines the mean precipitation, dotted area show months with water deficit (when the precipitation curve < temperature curve), area with vertical lines indicate the rainy season (precipitation > temperature), black areas indicate periods with > 100 mm rainfall. (For interpretation of the references to colour in this figure legend, the reader is referred to the web version of this article.)

are of crystalline base at the southern limit of the Ibiapaba plateau complex (Lemos and Meguro, 2010; Moro et al., 2016; Silva et al., 2017) with a predominant occurrence of lictolic Entisols (Santos et al., 2011, 2018; Soil Survey Staff, 2014). Climate in the dry-forest site is semi-arid (BSh), characteristic of hot steppes (Köppen, 1948) and with a smaller influence of the ITCZ (Andrade et al., 2017). Mean temperature ranges between 24° and 28 °C and the annual rainfall averages 560 mm, concentrated between January and April (Lemos and Meguro, 2010).

2.2. Climate data

For the correlations between growth and local climate variables, we used monthly precipitation between 1950 and 2019 data (Fig. 1) obtained from local meteorological stations near the study sites: for the evergreen-forest site from the municipality of Ubajara in Ceará state, for the savannah site from the municipalities of Piripiri and Piracuruca, Piauí state, and for the dry-forest site from the Aiuaba municipality, Ceará state. Data were obtained from the website of the Ceará Foundation for Meteorology and Water Resources - FUNCEME (www.funceme.br; Funceme, 2020) for the evergreen and dry-forest sites, and from the HIDROWEB platform (www.snirh.gov.br/hidroweb; ANA, 2020) for the savannah site. We confirmed the quality of the precipitation data for each of the stations by correlating average yearly precipitation values from the station with gridded reconstructions of precipitation over land and with gridded sea surface temperatures (Appendix Fig. S1). Monthly temperature data were unavailable at the meteorological stations and we used CRU TS v.4 (Harris et al., 2020) interpolated data for the cells corresponding to our sites, obtained from the KNMI Climate Explorer (https://climexp.knmi.nl; Trouet and Van Oldenborgh, 2013).

For the correlations between growth and global climate variables we used gridded Sea Surface Temperatures (SST) reconstructions and an El Niño Southern Oscillation (ENSO) index. For the SST reconstructions we used the National Center for Environmental Information SST reconstruction with optimal interpolation of 0.25° (Reynolds and Smith, 1994). To represent the ENSO, we used the El Niño 3 index that consists of ocean temperature anomalies in the Pacific between 90°–150°W and 5°N–5°S. We choose the monthly El Niño 3 index as a metric for the ENSO, after running spatial autocorrelation tests (trough KNMI Climate Explorer) with different ENSO indices and finding that the El Niño 3 showed the best results. El Niño 3 indices were obtained from the North American Monitoring Agency (NOAA; www.esrl.noaa.

gov/psd/forecasts/sstlim/timeseries).

To avoid problems that arise when using strongly correlated explanatory variables during analyses, we checked for correlations between local and global data (Appendix Fig. S2) and excluded combinations of strongly correlated climatic factors that may cause collinearity issues.

2.3. Selected species

Six tree species, three from the genus *Aspidosperma* and three from the genus *Handroanthus,* were selected based on the floristic collections of the studied sites (Araújo et al., 1999; Castello et al., 2018; Lemos and Meguro, 2010; Matos and Felfili, 2010; Moro et al., 2015; Silveira et al., 2020). In the evergreen-forest site we sampled *Aspidosperma castroanum* A.C.D. (Apocynaceae) and *Handroanthus serratifolius* (Vahl) S.Grose (Bignoniaceae), in the savannah site *Aspidosperma subincanum* Mart. and *Handroanthus ochraceus* (Cham.) Mattos, and in the dry-forest site *Aspidosperma multiflorum* A. DC. and *Handroanthus impetiginosum* (Mart. ex DC.) Mattos. These species are part of the 10 most abundant families of the *Caatinga* biome, are representative along the studied vegetation gradient and have high ecological and economic relevance for the region (Fernandes et al., 2020; Queiroz et al., 2017). In addition, recent studies have shown their suitability for dendrochronological studies (Andrade et al., 2019; Aragão et al., 2019; Espinosa et al., 2018; López and Villalba, 2020).

We also explored using species of another genus with potential for tree-ring analyses: the genus *Cordia* (Boraginaceae; Briceño-J et al., 2016) that occurs in two of our sites (*C. bicolor* in the evergreen forest, *C. trichotoma* in the dry forest). However, ring boundaries of these species were unclear and including them would require an in-depth exploration of their dendrochronological potential (e.g., Aragão et al., 2019) beyond the scope of this work. Although unsuccessful, we report this trial to register the failed attempt and stimulate further explorations on this widespread genus.

2.4. Dendrochronological analyses

Samples were collected in an opportunistic design by guided tour (Williams and Brown, 2019), in which individuals of various sizes (diameter at breast height between 9.5 and 35 cm) were selected along the areas of occurrence of populations of our intended species at each site. Using a gasoline-powered motorized drill (Stihl BT45) and hollow metal drills (external diameter ~25 mm), we collected between three and four radial samples per individual. These samples were approximately 15 mm in diameter and had varying lengths from bark to pith depending on the individual's diameter. We sampled 20 individuals in 3–4 radii of each species at each site, totalling 120 trees for the six species analysed. Broken samples were carefully aligned, and all samples were packed in paper bags, dried at room temperature, and fixed on wooden supports. Samples were then polished with increasingly finer sandpaper (grain from 60 to 2000) to allow for a good visualization of the ring boundaries under stereomicroscopy (Gärtner et al., 2015; Orvis and Grissino-Mayer, 2002). Some radial samples were also anatomically sectioned (Appendix Fig. S3) to describe the anatomy of the species and the ring boundaries (cf. Aragão et al., 2019). This procedure helps in understanding the species' growth-ring boundaries and aids in the identification of false rings common in tropical forests (Brienen et al., 2016).

Prior to measuring the tree rings, we observed and demarcated the growth layers under a Leica® stereomicroscope (amplification from 10x to 40x). Then we scanned samples with 2400 dpi resolution (EPSON Perfections V800 Photo Scanner) in ".tif" format. Ring widths from the 3–4 radii per individual were measured using CooRecoder and CDendro software (version 9.4 for Windows; Cybis, 2020) with an accuracy of 0.01 mm. We visually crossdated the ring-width series in CooRecorder, both within and between trees, aided by the correlation curves and skeleton plots in CDendro. Subsequently, we performed a statistical quality control of this crossdating using the COFECHA software (Holmes, 1983) to identify and solve possible marking errors. Chronologies were constructed for each site × species combination using the dplR package (Bunn et al., 2017) in software R version 3.6.3 (R Core Team, 2015). We detrended our radial series using flexible 22-year cubic splines with a 50% wavelength cut-off (Hughes et al., 2011; Speer, 2010) and chronologies were calculated from the detrended radial series. We then used the standard versions of each chronology, truncated to the years with a sampling depth of at least 10 radii, for the subsequent climate-growth analyses. As the rainy season – and thus the growing season – nearly coincides with the calendar year in Northeastern Brazil, we did not apply the Shulman shift (Schulman, 1956) to our chronologies. We calculated the standard dendrochronological statistics (cf. Hughes et al., 2011) related to the quality of the chronologies: the mean of the within-tree inter-series correlations (intercor); the between-tree inter-series correlation (rbar), and the Expressed Population Signal (EPS).

To explore the relationship between growth and local climate, initially we correlated growth variation with total annual precipitation averages for all forests. Next we performed correlation function analyses between the chronologies, precipitation (from the nearest meteorological stations) and temperature data (interpaled data obtained in KNMI) for each location using the *treeclim* R package (Zang and Biondi, 2015). To account for possible effects of pre-rainy season precipitation on growth (Aragão et al., 2019; Nogueira Jr et al., 2017; Pereira et al., 2018), or of legacy effects of drought events (Kannenberg et al., 2020), we applied monthly correlations starting from the November of the year preceding ring formation to July of the year of ring formation.

We then explored the relationship between growth and global sea surface temperature (SST) reconstructions to identify which regions of the ocean affect tree growth in our sites. We produce correlation maps between all chronologies and global SST reconstructions using the KNMI Climate Explorer (Trouet and Van Oldenborgh, 2013). In order to account for the autocorrelation in the data and contemplate possible delays in growth responses in each site (Aragão et al., 2019; Land et al., 2017), SST-growth correlations were performed month using running means with differing number of months between sites. The length of the running means coincided with the length of the rainy season of each site along the gradient: 9 months in evergreen forest (nov-JUL), 8 months in savannah (nov-JUN), and 7 months in dry forest (nov-MAY).

To validate the results of the SST correlation maps, we performed correlation function analyses between the chronologies and monthly values of the El Niño 3 index (representing the El Niño Southern Oscillation) in the *treeclim* R package (Zang and Biondi, 2015). As SSTs in different Atlantic Ocean regions may affect tropical tree growth (Aragão et al., 2019; Schöngart et al., 2017), we ran additional explorative analyses correlating growth and indices of different Tropical Atlantic regions: the Tropical North Atlantic index (TNA), Tropical South Atlantic index (TSA) and Western Hemisphere Warm Pool (WHWP) index (Appendix Tables S1 and S2).

To identify the combination of months in which growth variation responded significantly to climate, we applied both simple and multiple linear regression models (Hughes et al., 2011; Speer, 2010). The combination of single and multiple regression models helps in understanding growth variation in more detail (Hughes et al., 2011) and allow unravelling the relationships between chronologies and climatic variability (Aragão et al., 2019; Nogueira Jr et al., 2017). We performed regressions between growth and each of the three main climatic variables: growth vs. monthly precipitation, growth vs. monthly temperature, and growth vs. monthly Niño 3 index. Analyses were performed using the months comprising the rainy season of each site, varying between 7 and 9 months as described above. Model selection was performed using the backward method. All climate-growth correlations and the simple and multiple regressions were calculated over the period starting from 1957 or 1984 (variable according to chronologies) to

2019, using the software R 3.6.3 (R Core Team, 2015).

To understand how growth sensitivity to climate is modulated by the gradient, we tested whether the relationship between growth and climatic variables changed between the locations (testing for differences in the climatic-response slopes) as well as checking whether the explanatory power of the models (the R^2) changed along the gradient. For each climatic dataset (precipitation, temperature, and El Niño 3 index) we first applied a multiple linear regression model between growth and seasonal climatic data and tested within genera whether site was a significant factor in the regressions (including site as a factor in the regression). Next, we tested whether relationships were different between genera within sites. With this approach we thus test whether slopes change along the gradient as well as testing whether site conditions are a stronger determining factor of the climate-growth relationships than genera (thus overriding differences between genera). To allow for intercomparisons of slopes and R^2 values between species, we performed these analyses over the common period of 1984–2018. Seasonal values of climate were computed using the months comprising the rainy season of each site, varying between 7 and 9 months as described above.

2.5. Growth deviation analyses

To understand growth anomalies for our species, we identified years with positive and negative growth deviations (i.e., pointer-year analyses) for each species. The method to identify pointer years uses 4-year moving windows applied to the non-detrended, absolute growth data for each radii (Schweingruberl et al., 1990; van der Maaten-Theunissen et al., 2015). Pointer years are identified as growth deviations relative to the average growth rate of the four preceding years: positive pointer years are those when at least 75% of the tree-ring series show a growth increase of at least 60% (relative to the preceding 4 years); negative pointer years are those when > 75% of the trees show a > 40% growth reduction (cf. Schweingruberl et al., 1990). These analyses were performed on the individual radii over the common periods of 1963–2019 for the *Aspidosperma* species and 1975–2019 for *Handroanthus* species. Common periods were chosen to include at least 35 radii – equivalent to ~10 individuals – for every species per genus.

To explore which environmental variables drive the growth deviations, we checked whether growth deviations occurred during years of specific climatic deviations (e.g., dry years, El Niño or La Niña years, etc.) described in the literature (Jimenez et al., 2019; Marengo et al., 2012; Utida et al., 2019). The low number of pointer years in our data, however, hampered formally testing this relationships. Finally, we also explored resilience components (resilience, recovery, resilience and relative resilience) for the years with significant negative growth deviations (in least 5 radii) using 4-year windows (before and after; van der Maaten-Theunissen et al., 2015). For the growth-deviation and resilience-component analyses we used the *pointRes* package in R 3.6.3 (R Core Team, 2015; van der Maaten-Theunissen et al., 2015).

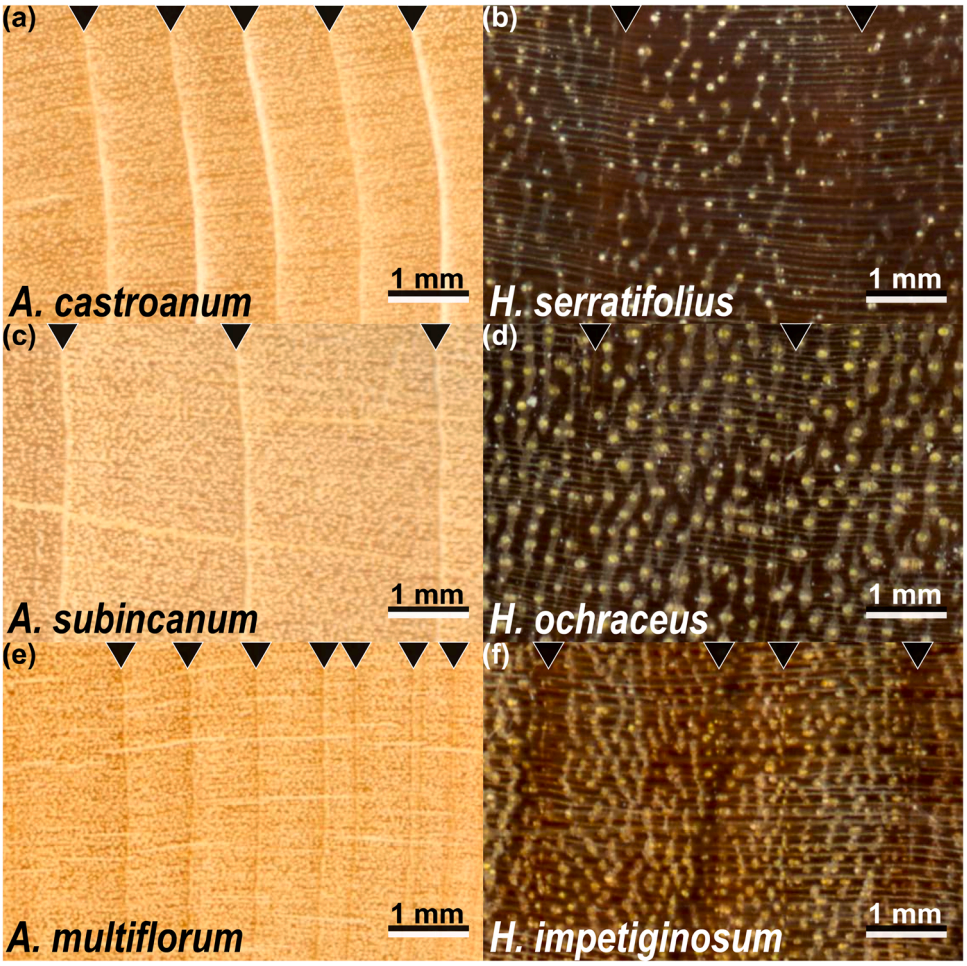

Fig. 2. Macroscopic transverse images of the wood of the 2 × 3 congeneric species studied: 2 genera (*Aspidosperma* and *Handroanthus*) in three forest types: evergreen forest; neotropical savannah (*Cerrado*); tropical dry forest (*Caatinga*). True ring boundaries are indicated by black triangles.

3. Results

3.1. Ring boundaries and tree-ring measurements

Growth-ring boundaries of the species of the genus *Aspidosperma* (Fig. 2a, c and e) were visible with a magnifying glass with 10x amplification, while the rings of species of the *genus Handroanthus* (Fig. 2b, d and f) were visible only under a stereomicroscope (Fig. 2). The genus *Aspidosperma* shows growth rings delimited by a thin line of marginal parenchyma, thick-walled latewood fibers and differences in vessel diameters: larger vessels in the earlywood and smaller vessels (spaced further apart) in the latewood (Appendix Fig. S3a, c and e). The genus *Handroanthus* presented rings characterized by a marginal parenchyma line (sometimes absent) and dark fibrous zones with a low vessel density (Appendix Fig. S3b, d and f). False rings were observed in all species, consisting mainly of variations in wood colour, fibrous zones, and confluent aliform axial parenchyma. In species of the genus *Aspidosperma* false rings were characterized by a narrow row of cells forming irregular and discontinuous layers or by abrupt variations in wood colour and density. Species of the genus *Handroanthus* presented false rings associated with the confluence of aliform parenchyma, which were visually distinct from the marginal parenchyma line delimiting true growth rings. Wedging ring – lens shaped rings that converge at some parts of the tree's circumference becoming absent in some radii – were present in both species, but mostly in the genus *Handroanthus*. For both species, the anatomical differences between false and true ring boundaries allowed us to correctly identify them during measurements and crossdating.

Crossdating and chronology building was successful for all species × site combinations. We were able to match the growth of most broken samples (lacking bark or pith) and we only disregarded a small number of radii (~10%) due to anomalous growth patterns (approximately 6–8 radii per species, with up to three trees excluded). Maximum tree ages varied between species from 48 to 77 years and the chronologies spanned between 41 and 67 radii (Fig. 3; Table 1). In all study species, clear growth synchrony was observed: chronologies presented inter-series correlations (intercor) ranging from 0.559 and 0.641, between-tree inter-series correlation (rbar) of 0.269 CE.334, and EPS values between 0.851 and 0.966 (Table 1). For species of the genus *Aspidosperma*, rbar increased with increasing drought while for *Handroanthus* species, this pattern was not observed.

3.2. Local climate-growth correlations

For all species, growth correlated positively with total annual precipitation for all six study species (r between 0.51 and 0.77; Appendix Fig. S5) and with monthly precipitation for the period around the growing season of each site (Fig. 4 and Table 2; Appendix Tables S1 and S2). The two evergreen-forest species exhibited the largest number of monthly correlations with rainfall (7 months; Fig. 4), while at the savannah and dry-forest site the number of months was lower (~4 months; Fig. 4 and Table 2; Appendix Tables S1 and S2). Through multiple linear regressions we identified that precipitation in months of January and May were the strongest determinants of growth (Fig. 4, Table 2). Among the growing season correlations, precipitation affected tree rings to a greater proportion in dry forests (Fig. 4, asterisks). In *A.*

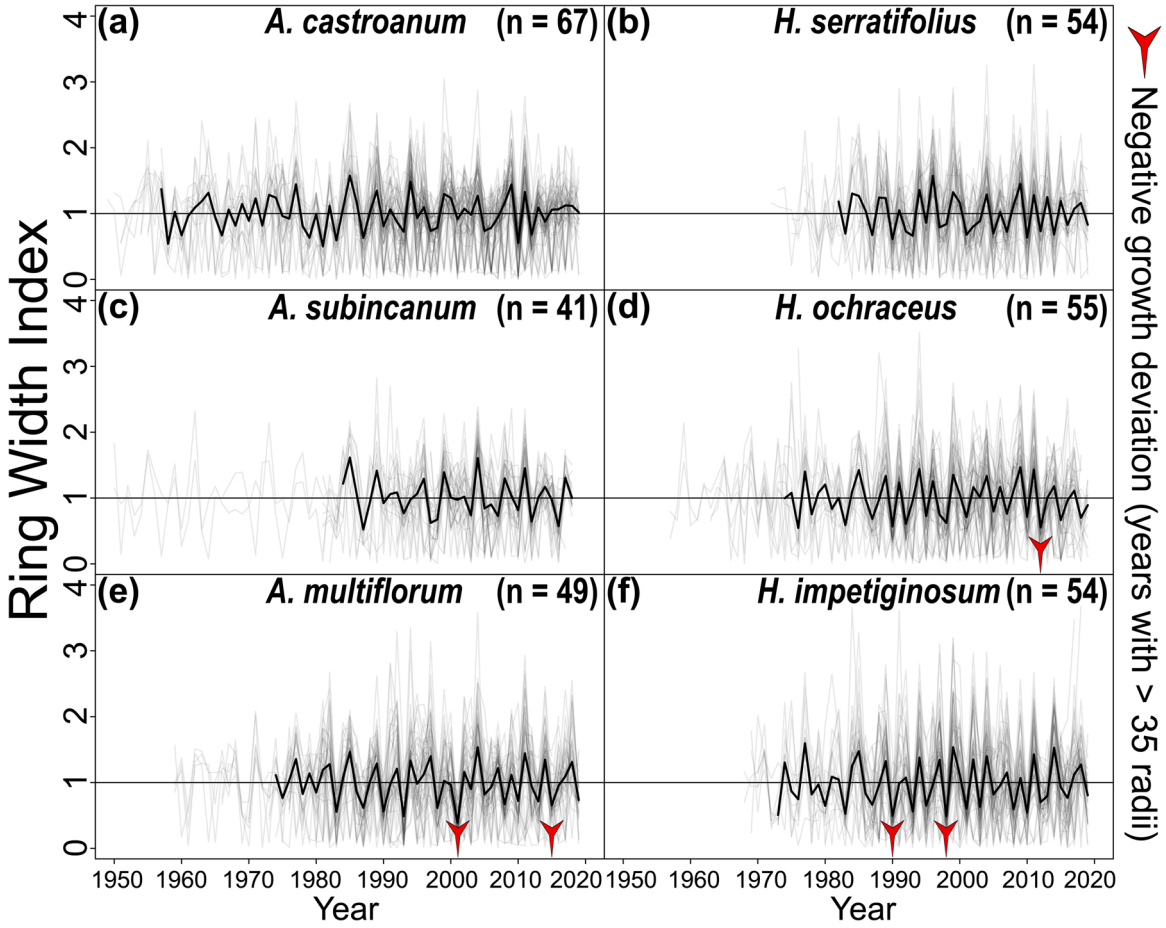

Fig. 3. Ring-width chronologies of 6 species belonging to two genera (*Aspidosperma* and *Handroanthus*) and studied at three sites: evergreen-forest; neotropical savannah (*Cerrado*); tropical-dry forest (*Caatinga*). Shown are the standardized series of individual trees (gray lines), the resulting average ring-width chronologies (black line) and years with significant negative growth deviations (downward arrows).

Table 1
Characteristics of chronologies for 6 species belonging to two genera (*Aspidosperma* and *Handroanthus*) at three study forest types: EF: Evergreen-forest; SA: Neotropical savannah site (*Cerrado*); TD: tropical-dry forest (*Caatinga*).

Species (forest types)	# trees (series)	intercor	Rbar	EPS	Mean age (max)	Mean ϕ (max)	Span
A. castroanum (EF)	20 (67)	0.619	0.277	0.938	63 (71)	12.5 (19.7)	1957–2019
A. subincanum (SA)	17 (41)	0.596	0.269	0.851	35 (68)	15.4 (34.4)	1984–2018
A. multiflorum (TD)	17 (49)	0.641	0.292	0.934	46 (61)	10.6 (12.7)	1974–2019
H. serratifolius (EF)	20 (54)	0.559	0.334	0.946	38 (48)	19.1 (27.2)	1982–2019
H. ochraceus (SA)	20 (55)	0.585	0.275	0.966	46 (77)	15.9 (28.0)	1974–2019
H. impetigisonus (TD)	20 (54)	0.603	0.310	0.947	47 (62)	14.6 (33.7)	1973–2019

Included are number of trees in the chronology (number of radii in parentheses); intercor: mean of the within-tree inter-series correlations; rbar: between-tree inter-series correlation; EPS: Expressed Population Signal; average (and maximum) tree ages; ϕ: average (and maximum) tree diameters; Span: beginning and end years of the chronologies.

multiflorum we observed the greatest proportional effect of precipitation (75%), where 3 of the 4 correlated months are determinant for growth (Fig. 4 and Table 2; Appendix Tables S1 and S2).

For all species, growth correlated negatively with monthly maximum temperature for the period around the growing season of each site (r between −0.30 and −0.55; Fig. 4 and Table 2; Appendix Tables S1 and S2). The two evergreen-forest species exhibited the largest number of monthly correlations with maximum temperature (~5 months; Fig. 4 and Table 2; Appendix Tables S1 and S2), while at the savannah and dry-forest site the number of months with correlations was lower (~3 months; Fig. 4). Even with the high number of correlations, we did not observe significant effects of maximum temperature on the growth of the six species through multiple regressions (Fig. 4 and Table 2; Appendix Tables S1 and S2).

3.3. Sea surface temperatures and El Niño

The correlation maps between the chronologies and global sea surface temperatures (SST) showed that the main ocean area affecting the growth of our study species is the Equatorial Pacific Ocean (Fig. 5). Correlations with tropical Pacific Ocean SSTs were strongest (higher correlation coefficients over larger areas) for evergreen forest and savannah species (Fig. 5 upper and central rows), and weaker for the dry forest species (Fig. 5, lower row). In general, results from the correlation maps were corroborated by the correlations with the El Niño 3 index, revealing negative correlations for all species. In the multiple regressions, the El Niño 3 index was a significant factor affecting tree growth for the savannah and dry-forest sites, with the strongest regression coefficients found for the savannah species (Fig. 4; Table 2; Appendix Tables S1 and S2). Evergreen forest species showed no significant El Niño 3 effects in the multiple regressions (Fig. 4; Table 2; Appendix Tables S1 and S2). Atlantic Ocean SSTs also affected growth variability of our species (Fig. 5), but results varied between species. In general, growth correlated negatively with Atlantic Ocean SSTs (these results are corroborated by the correlation analyses between growth and Atlantic Ocean SST indices, see Appendix Tables S1 and S2).

3.4. Site versus genus driving growth-variation

Species of the distinct genera occurring within the same site showed growth synchronicity, with the strongest Pearson's correlation of 0.87 for the two species in the dry-forest site (Appendix Fig. S4). When compared among sites, growth of the two dry-forest species correlated among themselves, but not with species (congeneric or not) from the evergreen forest or savannah (Appendix Fig. S4). Growth of the four species from the evergreen forest and the savannah showed synchronicity, correlating significantly between themselves (Pearson's r between 0.64 and 0.78) for all but one species combination (*A. subicanum* with *A. castroanum*).

When testing whether site was a stronger driver of growth synchronicity than genus, we found evidence that site indeed drives (or explains) growth variability more than the similarity within congeneric species. In addition, we also observed differences between growth responses to precipitation across rainfall gradient in both genera (Fig. 4). The precipitation-growth regressions showed a positive effect of precipitation on growth for all sites and a significantly different slope for both dry-forest species compared to the others (Fig. 6). For maximum temperature and El Niño 3 index we found no changes in the slopes across sites, with similar negative effects of temperature and El Niño on growth in all cases.

3.5. Growth deviations: pointer year analyses

The growth deviation analyses showed both positive and negative deviations (Appendix Fig S6). Three out of the six species studied showed significant growth decreases: in the dry forest *A. multiflorum* (Fig. 1e; Appendix Figs. S5 and S6a) and *H. impetiginosum* (Fig. 1f; Appendix Figs. S5f and S6b), in the savannah *H. ochraceus* (Fig. 1d; Appendix Figs. S5 and S6a). Most growth deviations were found for dry-forest species (5 negative and 1 positive; Appendix Fig S5), and the strongest reduction was found for *A. multiflorum*, which showed 89% negative growth deviation in 2001 (Appendix Figs. S6, S7a and Table S5).

The analysis of resilience components revealed that *A. multiflorum* (dry forest) showed two growth reductions (in 2001 and 2015), with the lowest relative resilience in 2015 (about 30%; Appendix Fig. S7 and Table S5). *H. impetiginosum* (dry forest) showed a significant reduction in growth in 1990 and 1998, with similar variations in resilience components and relative resilience of about 63% for both years (Appendix Fig. S7b and Table S5). *H. ochraceus* (savannah) showed a significant reduction in growth in 2012, with the smallest relative resilience between all species (about 22%; Appendix Fig. S7b and Table S5).

4. Discussion

This is one of the first evaluations of growth responses to climatic variability across a gradient of seasonally dry tropical forest types. Across vegetation types and species, we found consistent positive effects of rainfall on growth and negative effects of temperature. Yet, the magnitude of these effects differed across vegetation types and was strongest in the driest type (dry forest).

4.1. Growth synchronicity and local climatic drivers

The six species presented different types of ring boundaries (Brienen et al., 2016; Fichtler and Worbes, 2012), which coincided with the descriptions of other studied species of the genera *Aspidosperma* (Aragão et al., 2019; Aragão and Lisi, 2019; López and Villalba, 2020) and *Handroanthus* (Andrade et al., 2019; Espinosa et al., 2018; Pace et al., 2015). Anatomical characterization of the growth ring boundaries using histological sections reduced identification errors during the measurements and aided in the construction of chronologies (Aragão et al., 2019; Brienen et al., 2016; López and Villalba, 2020). The high synchronization between our series and the inclusion of most sampled radii per

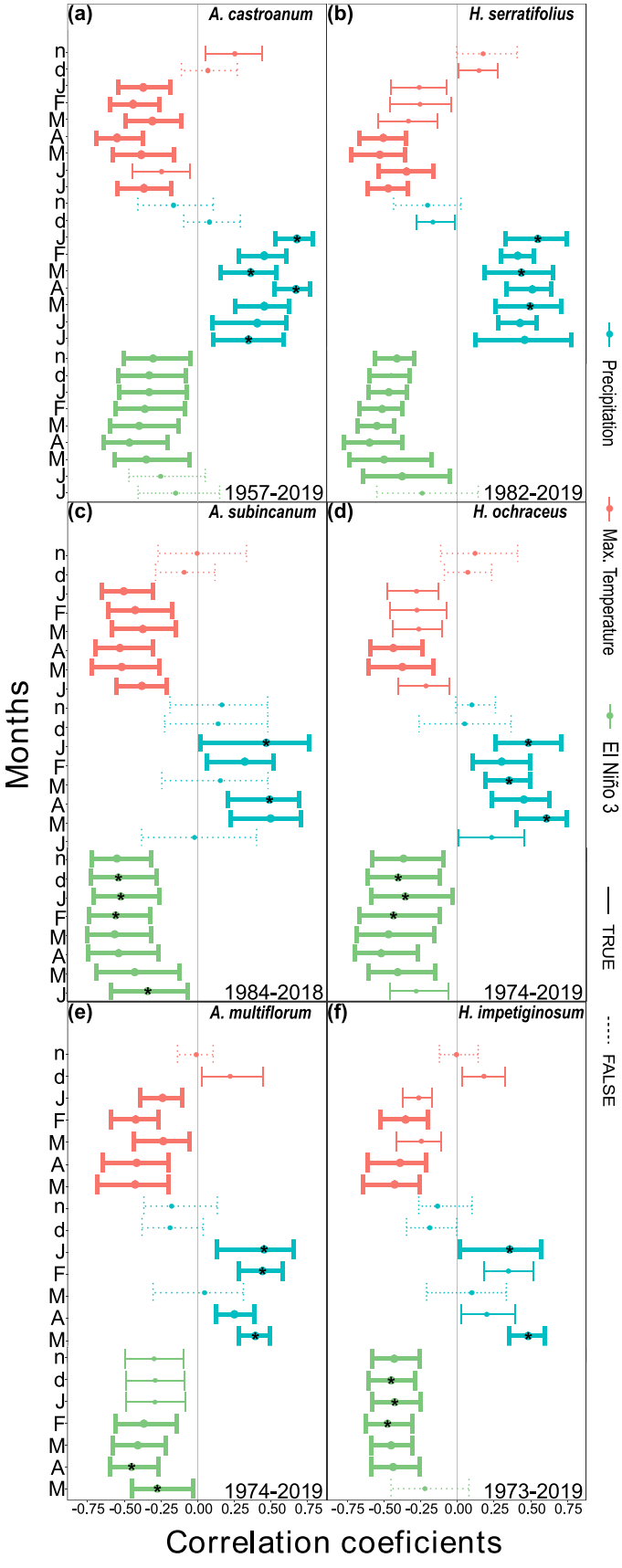

Fig. 4. Climate-growth correlations and multiple-regression for six species belonging to two genera (*Aspidosperma* and *Handroanthus*) at three study sites: evergreen-forest; neotropical savannah (*Cerrado*); tropical-dry forest (*Caatinga*). Growth was compared to monthly precipitation (red), maximum monthly temperatures (blue) and the El Niño 3 index (green). Months of the previous year are indicated in lowercase letters, while those of the current year in uppercase. Central dots indicate the correlation coefficients and the lines the bootstrapped 95% confidence intervals: full lines show significant correlations, dashed lines not significant. Thick lines indicate $p < 0.05$ under simple regression and the * in the centre of the lines indicate the months had a significant effect on growth ($p < 0.05$) in best model under multiple regression. (For interpretation of the references to colour in this figure legend, the reader is referred to the web version of this article.)

Table 2
Results of multiple regression analyses for each species between the chronology (dependent variable) and historical monthly mean values of local (precipitation) and global (El Niño Southern Oscillation) environmental variables.

	Species	Variables	b ± SE	Species	Variables	b ± SE
Evergreen forest	*A. castroanum* 1. $R^2 = 0.65$ (F = 27.47; df = 57)	Intercept	0.4785 ± 0.0634 * **	*H. serratifolius* 1. $R^2 = 0.51$ (F = 11.82; df = 37)	Intercept	0.479 ± 0.1036 * **
		Prec. Jan	0.0011 ± 0.0002 * **		Prec. Jan	0.0011 ± 0.0003 * **
		Prec. Mar	0.0003 ± 0.0002 * **		Prec. Mar	0.0006 ± 0.0003 *
		Prec. Apr	0.0005 ± 0.0002 * **		Prec. May	0.0007 ± 0.0003 *
		Prec. Jul	0.0012 ± 0.0006 * **			
Savannah	*A. subincanum* 1. $R^2 = 0.36$ (F = 9.11; df = 32)2. $R^2 = 0.49$ (F = 7.13; df = 32)	Intercept	0.5963 ± 0.1072 * **	*H. ochraceus* 2. $R^2 = 0.43$ (F = 10.48; df = 43)	Intercept	0.3994 ± 0.0862 * **
		Prec. Jan	0.0009 ± 0.0004 * **		Prec. Jan	0.001 ± 0.0003 * **
		Prec. Apr	0.0008 ± 0.0003 * **		Prec. Feb	0.0008 ± 0.0002 * **
		Intercept	9.9499 ± 1.9507 * **		Prec. May	0.0014 ± 0.0003 * **
		El Niño 3 Jan	0.7731 ± 0.3037 * **		Intercept	7.5099 ± 1.3731 * **
		El Niño 3 Feb	-0.4461 ± 0.1942 * **		El Niño 3 Jan	0.9458 ± 0.2173 * **
		El Niño 3 Jun	-0.1312 ± 0.0544 * **		El Niño 3 Feb	-0.6875 ± 0.1606 * **
		El Niño 3 dec	-0.5356 ± 0.1889 * **		El Niño 3 dec	-0.5002 ± 0.131 * **
Dry forest	*A. multiflorum* 2. $R^2 = 0.28$ (F = 8.52; df = 43)	Intercept	0.6162 ± 0.0669 * **	*H. impetigisonum* 2. $R^2 = 0.33$ (F = 7.65; df = 46)	Intercept	0.7343 ± 0.0624 * **
		Prec. Jan	0.001 ± 0.0003 * **		Prec. Jan	0.0009 ± 0.0004 * **
		Prec. Feb	0.0016 ± 0.0004 * **		Prec. May	0.0033 ± 0.0009 * **
		Prec. May	0.0028 ± 0.0008 * **		Intercept	7.2033 ± 1.4581 * **
		Intercept	6.983 ± 1.6506 * **		El Niño 3 Jan	0.6091 ± 0.2327 * **
		El Niño 3 Apr	-0.4903 ± 0.1366 * **		El Niño 3 Feb	-0.5291 ± 0.1697 * **
		El Niño 3 May	0.2766 ± 0.1183 * **		El Niño 3 dec	-0.3127 ± 0.1365 * **

Environmental variables and R2 values of two sets of models per species are provided: the first indicates values related to multiple regressions of growth vs. monthly precipitation and the second (only presented when significant) of models related to growth vs. monthly El Niño 3 indices. Multiple regression coefficient b and standard error are provided, significance levels indicated as * $p < 0.05$ and * ** $p < 0.001$

species indicate we have robust chronologies with high measurement accuracy (Brienen et al., 2016; Worbes, 2010).

Although the genera belong to different families (Fernandes et al., 2020; Queiroz et al., 2017), local climatic drivers of growth were consistent across species and climates (Figs. 5 and 6). The strong correlations between our ring-width chronologies and monthly, seasonal and annual precipitation (Figs. 5 and 6; Appendix Fig S3) indicate that growth synchronicity is driven by water availability (Aragão et al., 2019; Brienen et al., 2016; López et al., 2019; Schöngart et al., 2017). Precipitation effects at our dry-forest site are similar to those obtained in other dry-forest studies (Aragão et al., 2019; Lisi et al., 2020; López et al., 2019; López and Villalba, 2020), while at our evergreen-forest site precipitation effects were stronger than those found at similar forest types (Fontana et al., 2018; Granato-Souza et al., 2018). These higher growth correlations suggest a stronger growth response to climate variability, and/or a higher interannual variability (IAV) in climate in our study region.

Ring-width chronologies for the dry forest species were not correlated to those of the other two sites. This lack of synchronicity points to differences in climate-growth responses across the vegetation types (Aragão et al., 2019; Babst et al., 2019; Lisi et al., 2020; López et al., 2019). It could also relate to differences in the synchronicity of precipitation variability between the dry-forest site and the two other sites (Appendix Fig. S8), as the savannah and evergreen forest sites are under stronger influence of the Intertropical Convergence Zone (ITCZ) than the dry-forest site (Andrade et al., 2017). The relationship between chronologies and precipitation (per genus and per location - Appendix Tables S3 and S4) corroborates that local climate is the main driving factor of these differences (Aragão et al., 2019; Babst et al., 2019; Lisi et al., 2020; López et al., 2019). These results also suggest that congeneric species can be used in comparative studies along environmental gradients as their growth IAV (Appendix Tables S3 and S4) does not differ within and between the genera (Locosselli et al., 2013). This result differs from the convergence in growth responses observed in other studies on the same species across environmental gradients (López et al., 2019; López and Villalba, 2020), and reveals differential responses to climate variability of tropical tree species growing in different vegetation types.

The higher dependence to rainfall in the dry forest suggest a stronger drought sensitivity and higher drought vulnerability of trees in this forest type, which is worrisome considering the increases in drought frequency forecast due to climate change (Kannenberg et al., 2020; Wang et al., 2016). If the responses for our study species are representative for dry forest tree species in general, our results may imply strong drought-induced fluctuations in carbon stocks and tree mortality in these forests (Allen et al., 2017). Continued efforts to quantify the heterogeneity in climate responses across species and forest types will help to better forecast drought impacts on tropical forests (Allen et al., 2017).

Although to a lesser extent, growth IAV was also affected by maximum temperature (T_{max}) along the gradient (Figs. 5 and 6; Appendix Table S1 and S2). These correlations may in part arise from the collinearity between precipitation and temperature, but negative growth responses to T_{max} are expected for tropical forests (Brienen et al., 2016) and have already been observed in other studies in the region (Nogueira Jr et al., 2017). In Northeastern Brazil (NEB), drought and high temperatures are common (Marengo et al., 2017; Pereira et al., 2014) and prolonged droughts can cause cumulative effects on tree growth, affecting growth over several years, and reducing the resilience of tree growth (Gao et al., 2018). Increases in temperature forecast in the future may further increase water stress in these forests and hence, increase the vulnerability of these forests to climatic extremes (Allen et al., 2017; Pennington et al., 2018). These changes may increase mortality, shift community compositions and reduce species richness (Allen et al., 2017).

4.2. Negative effects of the El Niño Southern Oscillation on growth

Of all the global SST variables affecting the growth IAV in our study sites, none was as strong as the El Niño Southern Oscillation (ENSO) events. SSTs in regions related to ENSO negatively influenced the IAV of

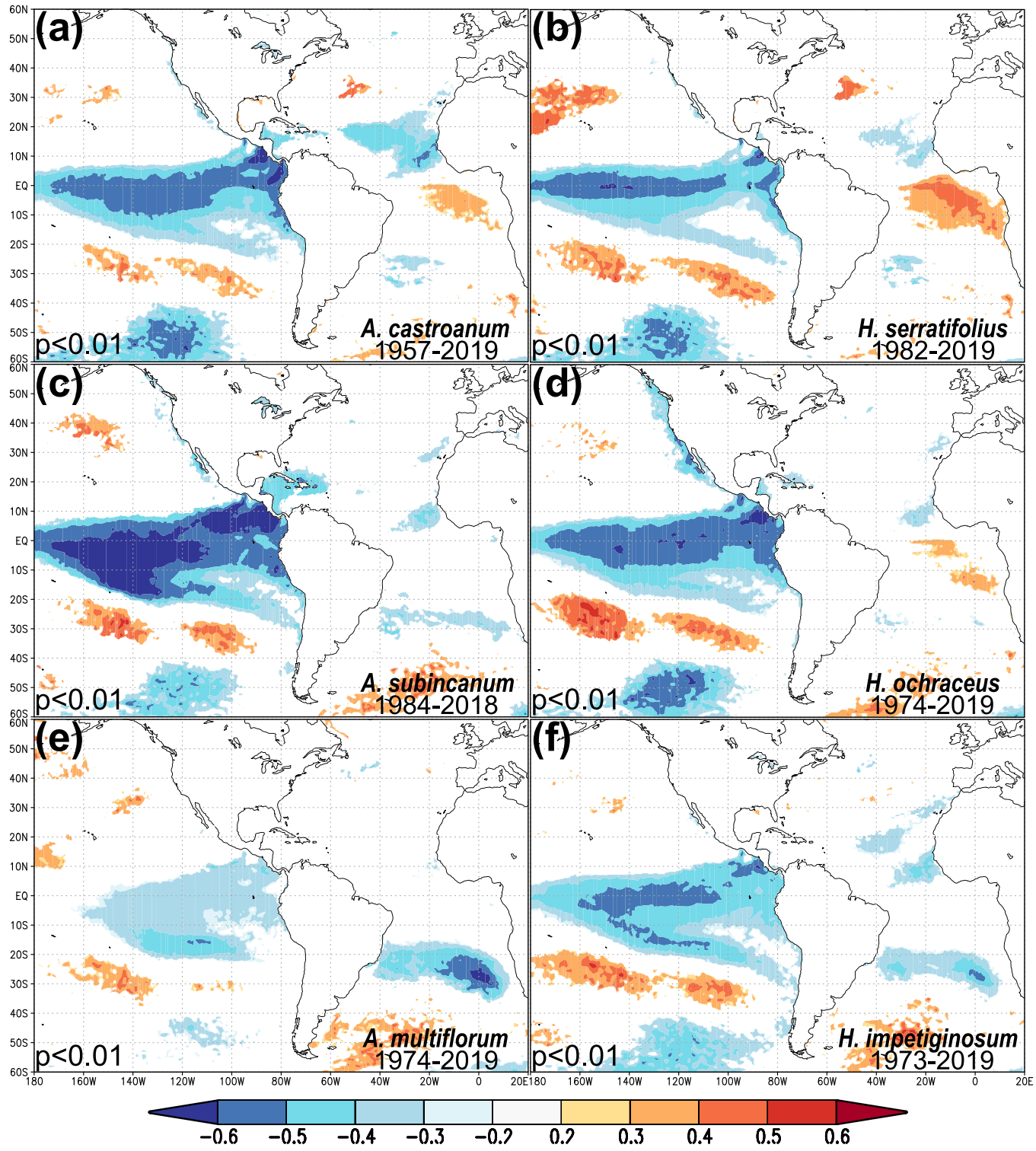

Fig. 5. Spatial correlations between monthly gridded sea surface (SSTs) temperatures in the Atlantic and Pacific oceans and the ring-width index chronologies for 6 species belonging to two genera (*Aspidosperma* and *Handroanthus*) at three study sites: Evergreen-forest; Neotropical savannah (*Cerrado*); tropical-dry forest (*Caatinga*). Grid data from the 0.25° optimal interpolation sea surface temperature reconstructions of the National Center for Environmental Information (Reynolds and Smith, 1994). Different running means were used corresponding to the growing season for each site: 9 months for the evergreen-forest site, 8 months for the savannah, and 7 months for the dry forest. Results are shown for the months with the highest correlations. Colours indicate Pearson's correlation coefficients.

the rings of all species along the gradient (Figs. 5–6 and Table 2). These results corroborate the strong effect of ENSO on tropical tree growth and growth IAV in the region (Aragão et al., 2019; Nogueira Jr et al., 2017). However, our multiple regressions suggest that the determining effect of ENSO occurred only in the savannah and dry forest (Figs. 5–6 and Table 2), with greater severity on *A. subincanum* and *H. impetiginosum* (savannah and dry forest, respectively).

The strong influence of precipitation and temperature on growth IAV are tied to the seasonality of rainfall in NEB, which in turn is strongly influenced by the position of the ITCZ (Jimenez et al., 2019; Marengo

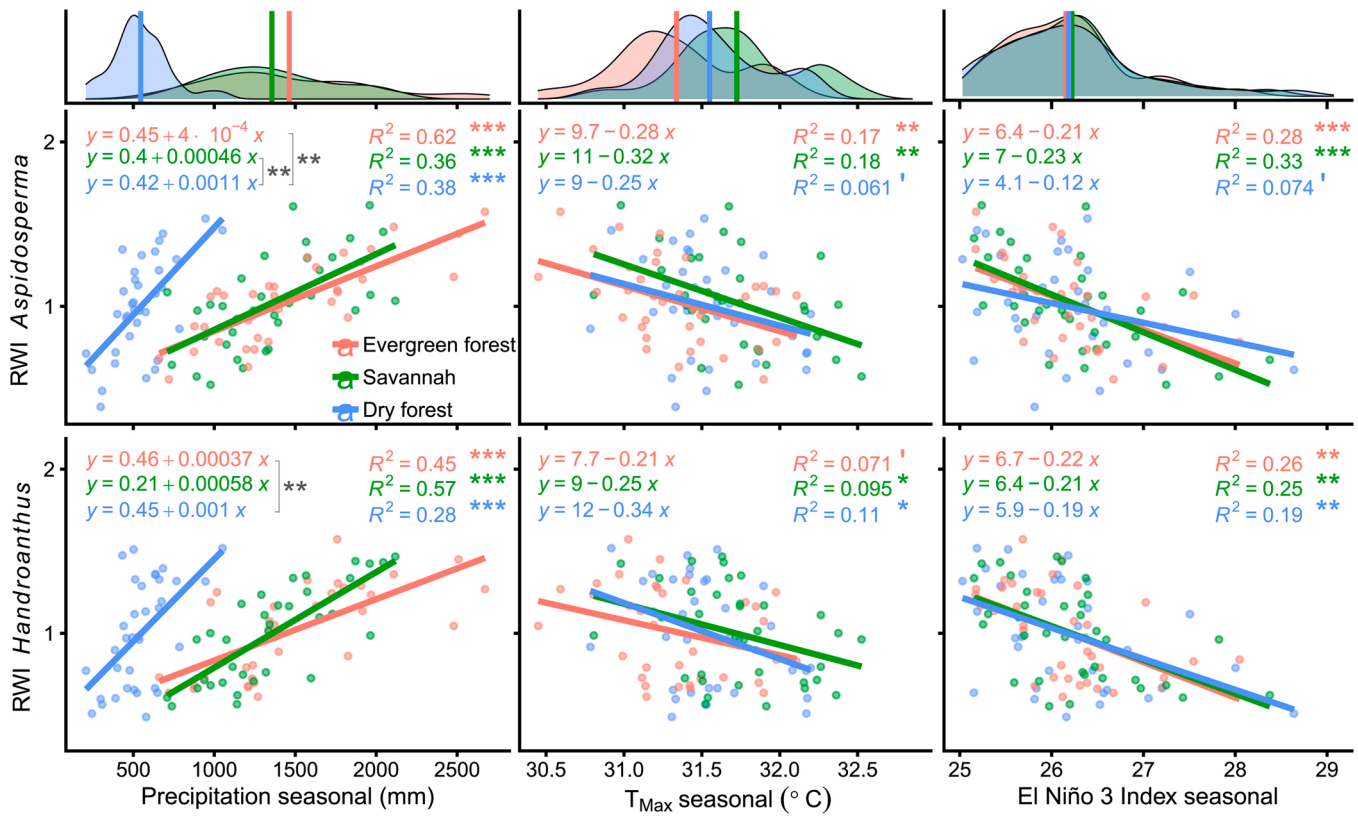

Fig. 6. Changes in climate-growth relations along a vegetation gradient in two genera (*Aspidosperma*, top; *Handroanthus*, bottom). Shown are linear regressions between ring-width chronologies (RWI) and growing-season precipitation (left), maximum temperature (Tmax; center) and El Niño 3 Index (right). Vegetation gradient indicated as: evergreen forest (red); neotropical savannah (*Cerrado*, green); tropical dry forest (*Caatinga*, blue). Regression equations, R-squared values, and p-values are shown. Grey asterisks indicate p-values for the test of site-effects on the regression slopes (* = $p < 0.05$, ** = $p < 0.01$, *** = $p < 0.001$). Growing season length: 9 months in the evergreen forest, 8 months in the savannah, and 7 months in the dry forest site. Climate data for 1984–2018 were used. (For interpretation of the references to colour in this figure legend, the reader is referred to the web version of this article.)

et al., 2017; Pereira et al., 2014). Atmospheric and oceanic factors, such as Sea Surface Temperatures (SST) alter the position and effects on local climate of the ITCZ (Correia Filho et al., 2019; Jimenez et al., 2019; Pereira et al., 2014; Wu et al., 2020). In general, growth IAV of our study species might thus reflect SST variations that affect NEB rainfall (Jimenez et al., 2019). More specifically, ENSO events are a major modulator of the ITCZ, thus reflecting the strong effect of ENSO on growth variability of NEB forests (Correia Filho et al., 2019; Jimenez et al., 2019; Pereira et al., 2020). Rainfall reductions during El Niño years thus drive the strong IAV in stem growth in seasonal forests, consequently affecting the IAV in carbon cycle of these forests (Linscheid et al., 2020; Zhao et al., 2018).

The responses to El Niño vary between species and between the different forests types in the region (Aragão et al., 2019; Nogueira Jr et al., 2019, 2017). These differences may be linked to phenological responses (Amorim et al., 2009), or to different strategies for using the water available for growth (Estrada-Medina et al., 2013). In seasonal environments, structural adaptations or drought-prevention strategies are common and water-use strategies vary between species (Butz et al., 2018). These characteristics can favor carbon gain, reduce water stress caused by drought and modulate growth (Estrada-Medina et al., 2013). Tradeoffs between reproduction and growth may also be under influence of ENSO events (Brodribb et al., 2020; Hogan et al., 2019) and may thus also drive these differences between species. Differences in growth responses between sites may relate to soil differences: savannah Entisols (sandy) and dry-forest litholic soils (FAO, 2014; Santos et al., 2011, 2018) show different water retention capacities. Shallow soils, and soils with low water retention capacity can exacerbate the negative drought effects caused by ENSO (Liu et al., 2020). In any case, we found that the savannah and dry forest regions are the most sensitive to the variations caused by El Niño. These results are worrisome considering the forecast increases in El Niño frequency due to climate change (Allen et al., 2017; Babst et al., 2019; Pennington et al., 2018; Silva et al., 2017).

4.3. Growth IAV in relation to Atlantic Ocean SSTs

Atlantic Ocean SSTs also influence the growth our species along the gradient (Fig. 5; Appendix Tables S1 and S2). Oscillations in Atlantic Ocean SSTs modulate the ITCZ position (Marengo et al., 2017) and are known to influence the growth of species in the region (Aragão et al., 2019; Nogueira Jr et al., 2019, 2017). According to climate change forecasts, these fluctuations will be even greater in the future (IPCC, 2014), with predicted reductions in rainfall and an increase in extreme drought events over NEB (Marengo et al., 2012). In sensitive systems such as dry forests, these scenarios are of concern, as they reduce the primary productivity of vegetation and increase the risk of collapse in the region's carbon sequestration (Ahlström et al., 2015; Frank et al., 2015).

4.4. Relative growth changes: pointer years

Results of our pointer-year analyses support evidence that growth reductions are linked to extreme drought events (Gao et al., 2018). Pointer years coincided with strong changes in Atlantic Ocean SSTs (*H. impetiginosum* in 1990 and *H. ochraceus* in 2012) or with the occurrence of severe El Niño events (*A. multiflorum* in 2015 and *H. impetiginosum* in 1998). Along with the reduced growth potential and resilience of drier vegetation, such events may cause (negative) legacy effects on growth in

subsequent years (Gao et al., 2018; Kannenberg et al., 2020). During drought, some vital functions of trees collapse and generate abrupt growth changes (Berdugo et al., 2020; Brodribb et al., 2020). Aridity can also damage the photosynthetic system, inhibit mycorrhizal interactions and reduce the resilience of trees to new drought events (Berdugo et al., 2020). Identifying indicator years helps in understanding how environmental factors influence species growth IAV and can thus assist in mitigation the impacts caused by them (Gradel et al., 2017b, 2017a).

An increase in growth sensitivity with increasing drought stress along the gradient is also corroborated by the larger number of pointer years observed for the species in the dry forest and savanna (Fig. 3, red arrows; Appendix Fig. S6 and Table S5). These growth reductions corroborate reductions found in the productivity of dry forests (Chen et al., 2019; Humphrey, 2021; Piao et al., 2020b) and suggest that dry-forests species are the ones that are most prone to growth loss during extreme years (Allen et al., 2017; Babst et al., 2019; Pennington et al., 2018; Silva et al., 2017). Extreme climatic events are forecast to increase in strength and frequency in the future (IPCC, 2014) and the growth reductions caused by these events are thus worrisome (Jimenez et al., 2019; Marengo et al., 2017, 2012; Utida et al., 2019), raising concerns about future increases in mortality risks of trees in these forests (Allen et al., 2010, 2017). Understanding the differential responses of different forest types to these events will be crucial for their proper management and conservation in the future (Banda-R et al., 2016; Pennington et al., 2018).

5. Conclusion

In conclusion, we proved the annual formation of tree rings for six species along a vegetation gradient in northeastern Brazil and showed their potential for the development of chronologies. Growth responses in the different types of seasonal forests (evergreen forest – savannah – dry forest) suggest that seasonal water availability is the main limiting factor of tree growth (Aragão et al., 2019; Babst et al., 2019; Lisi et al., 2020; López et al., 2019) and that tree growth is under strong modulating effect of global climatic phenomena such as El Niño events (Jimenez et al., 2019). Dry forests were the ones with the highest growth sensitivity to drought, and may therefore be more vulnerable to the effects of climate change (Allen et al., 2017; Brodribb et al., 2020).

Our tree-rings analyzes with congeneric species across a forest gradient proved to be effective. Although limited by idiosyncrasies in the growth patterns of each taxon, an approach using congeneric species amplifies the spatiotemporal scale of tree-growth variation studies. We found that site characteristics are the main modulators of tree-growth variability, overriding the effects of similarities within genera. Similar dendroecological studies can contribute to our understanding of the modulators of growth dynamics of tropical forests. Future studies should apply a similar approach over larger gradients and add additional environmental characteristics (e.g., soil) when analyzing growth variation in tree-rings. Understanding the sensitivity of different tropical forests to climate is key in understanding their carbon sequestration dynamics and potential. Studies like ours can thus be used to guide decision making on conservation measures of seasonally dry topical forests, especially under the scope of future climatic changes.

Declaration of Competing Interest

The authors declare that they have no known competing financial interests or personal relationships that could have appeared to influence the work reported in this paper.

Acknowledgements

We thank the managers of the conservation units and the local guides for the logistical support in the field, especially José and Mauro. We also thank friends and colleagues at the Dendroecology and Wood Biology Laboratory of the State University of Campinas, UNICAMP, Campinas-SP, Brazil. We thank Prof. Francisca Soares de Araújo from the Department of Biology of the Federal University of Ceará in Fortaleza, Brazil for receiving us, the great help in deciding field locations and the logistical support of sample collection by her project (CNPQ/ICMBIO/FAPs 18/2017 - Linha 1 - Caatinga CNPq #421350/2017-2). We also thank the logistical support and laboratory access granted to us by Prof. Mario Tommasielo Filho from the Luiz de Queiroz School of Agriculture, ESALQ-USP, Piracicaba-SP, Brazil. This study was funded by a Fundação de Amparo a Pesquisa do Estado de São Paulo (FAPESP) Young Investigator Grant (Process Number 2018/01847-0) granted to PG. JRVA received PhD scholarships from FAPESP (Process Number 2018/24514-7) and from the Coordenação de Aperfeiçoamento de Pessoal de Nível Superior - Brazil (CAPES; Process Number 88882.329278/2019-01). This work was carried out with the support of CAPES - Financing Code 001.

Appendix A. Supporting information

Supplementary data associated with this article can be found in the online version at doi:10.1016/j.dendro.2021.125913.

References

Ahlstrom, A., Raupach, M.R., Schurgers, G., Smith, B., Arneth, A., Jung, M., Reichstein, M., Canadell, J.G., Friedlingstein, P., Jain, A.K., Kato, E., Poulter, B., Sitch, S., Stocker, B.D., Viovy, N., Wang, Y.P., Wiltshire, A., Zaehle, S., Zeng, N., 2015. The dominant role of semi-arid ecosystems in the trend and variability of the land CO_2 sink. Science 348, 895–899. https://doi.org/10.1126/science.aaa1668.

Ahlström, A., Xia, J., Arneth, A., Luo, Y., Smith, B., 2015. Corrigendum: Importance of vegetation dynamics for future terrestrial carbon cycling. Environ. Res. Lett. 10, 1–10. ⟨https://doi.org/10.1088/1748-9326/10/8/089501⟩.

Allen, C.D., Macalady, A.K., Chenchouni, H., Bachelet, D., McDowell, N., Vennetier, M., Kitzberger, T., Rigling, A., Breshears, D.D., Hogg, E.H., (Ted), Gonzalez, P., Fensham, R., Zhang, Z., Castro, J., Demidova, N., Lim, J.-H., Allard, G., Running, S. W., Semerci, A., Cobb, N., 2010. A global overview of drought and heat-induced tree mortality reveals emerging climate change risks for forests. For. Ecol. Manag. 259, 660–684. https://doi.org/10.1016/j.foreco.2009.09.001.

Allen, K., Dupuy, J.M., Gei, M.G., Hulshof, C., Medvigy, D., Pizano, C., Salgado-Negret, B., Smith, C.M., Trierweiler, A., Van Bloem, S.J., Waring, B.G., Xu, X., Powers, J.S., 2017. Will seasonally dry tropical forests be sensitive or resistant to future changes in rainfall regimes? Environ. Res. Lett. 12, 023001 https://doi.org/10.1088/1748-9326/aa5968.

ANA, A.N. das Á., 2020. Séries históricas - HIDROWEB [WWW Document]. URL ⟨http://www.snirh.gov.br/hidroweb/serieshistoricas⟩.

Amorim, I.L., de Sá Barreto Sampaio, E.V., de Lima Araújo, E., 2009. Fenologia de espécies lenhosas da caatinga do Seridó, RN. Revista Árvore 33 (3), 491–499. https://doi.org/10.1590/S0100-67622009000300011.

Andrade, E.M., Aquino, D. do N., Chaves, L.C.G., Lopes, F.B., 2017. Water as capital and its uses in the Caatinga. In: Silva, J.M.C. da, Leal, I.R., Tabarelli, M. (Eds.), Caatinga. Springer International Publishing, Cham, pp. 281–302. https://doi.org/10.1007/978-3-319-68339-3_10.

Andrade, V.H.F., Machado, S. do A., Figueiredo Filho, A., Botosso, P.C., Miranda, B.P., Schöngart, J., 2019. Growth models for two commercial tree species in upland forests of the Southern Brazilian Amazon. For. Ecol. Manag. 438, 215–223. https://doi.org/10.1016/j.foreco.2019.02.030.

Anning, A.K., Rubino, D.L., Sutherland, E.K., McCarthy, B.C., 2013. Dendrochronological analysis of white oak growth patterns across a topographic moisture gradient in southern Ohio. Dendrochronologia 31, 120–128. https://doi.org/10.1016/j.dendro.2012.10.002.

Aragão, J.R.V., Groenendijk, P., Lisi, C.S., 2019. Dendrochronological potential of four neotropical dry-forest tree species: climate-growth correlations in northeast Brazil. Dendrochronologia 53, 5–16. https://doi.org/10.1016/j.dendro.2018.10.011.

Aragão, J.R.V., Lisi, C.S., 2019. Caatinga tree wood anatomy: perspectives on use and conservation. Floresta Ambient. 26. https://doi.org/10.1590/2179-8087.099717.

Araújo, F.S., de, Martins, F.R., Shepherd, G.J., 1999. Variações estruturais e florísticas do carrasco no planalto da Ibiapaba, estado do Ceará. Rev. Bras. Biol. 59, 663–678. https://doi.org/10.1590/S0034-71081999000400015.

Asmerom, Y., Baldini, J.U.L., Prufer, K.M., Polyak, V.J., Ridley, H.E., Aquino, V.V., Baldini, L.M., Breitenbach, S.F.M., Macpherson, C.G., Kennett, D.J., 2020. Intertropical convergence zone variability in the Neotropics during the Common Era. Sci. Adv. 6, eaax3644 https://doi.org/10.1126/sciadv.aax3644.

Babst, F., Bodesheim, P., Charney, N., Friend, A.D., Girardin, M.P., Klesse, S., Moore, D.J. P., Seftigen, K., Bjo, J., Dietze, M.C., Eckes, A.H., Enquist, B., Frank, D.C., Mahecha, M.D., Poulter, B., Record, S., Trouet, V., Turton, R.H., Zhang, Z., Evans, M. E.K., 2018. When tree rings go global: challenges and opportunities for retro- and prospective insight. Quat. Sci. Rev. 20.

Babst, F., Bouriaud, O., Poulter, B., Trouet, V., Girardin, M.P., Frank, D.C., 2019. Twentieth century redistribution in climatic drivers of global tree growth. Sci. Adv. 5, eaat4313 https://doi.org/10.1126/sciadv.aat4313.

Banda-R, K., Delgado-Salinas, A., Dexter, K.G., Linares-Palomino, R., Oliveira-Filho, A., Prado, D., Pullan, M., Quintana, C., Riina, R., Rodríguez, M., Weintritt, G.M., Acevedo-Rodríguez, J., Adarve, P., Álvarez, J., Aranguren B, E., Arteaga, A., Aymard, J.C., Castaño, G., Ceballos-Mago, A., Cogollo, N., Cuadros, Á., Delgado, H., Devia, F., Dueñas, W., Fajardo, H., Fernández, L., Fernández, Á., Franklin, M.Á., Freid, J., Galetti, E.H., Gonto, L.A., González-M, R., Graveson, R., Helmer, R., Idárraga, E.H., López, Á., Marcano-Vega, R., Martínez, H., Maturo, O.G., McDonald, H.M., McLaren, M., Melo, K., Mijares, O., Mogni, F., Molina, V., Moreno, D., Nassar, N. del P., Neves, J.M., Oakley, D.M., Oatham, L.J., Olvera-Luna, M., Pezzini, A.R., Dominguez, F.F., Ríos, O.J.R., Rivera, M.E., Rodríguez, O., Rojas, N., Särkinen, A., Sánchez, T., Smith, R., Vargas, M., Villanueva, C., Pennington, R.T, B., 2016. Plant diversity patterns in neotropical dry forests and their conservation implications. Science 353, 1383. https://doi.org/10.1126/science.aaf5080.

Bastos, A., Friedlingstein, P., Sitch, S., Chen, C., Mialon, A., Wigneron, J.-P., Arora, V.K., Briggs, P.R., Canadell, J.G., Ciais, P., Chevallier, F., Cheng, L., Delire, C., Haverd, V., Jain, A.K., Joos, F., Kato, E., Lienert, S., Lombardozzi, D., Melton, J.R., Myneni, R., Nabel, J.E.M.S., Pongratz, J., Poulter, B., Rödenbeck, C., Séférian, R., Tian, H., van Eck, C., Viovy, N., Vuichard, N., Walker, A.P., Wiltshire, A., Yang, J., Zaehle, S., Zeng, N., Zhu, D., 2018. Impact of the 2015/2016 El Niño on the terrestrial carbon cycle constrained by bottom-up and top-down approaches. Philos. Trans. R. Soc. B Biol. Sci. 373, 20170304 https://doi.org/10.1098/rstb.2017.0304.

Berdugo, M., Delgado-Baquerizo, M., Soliveres, S., Hernández-Clemente, R., Zhao, Y., Gaitán, J.J., Gross, N., Saiz, H., Maire, V., Lehmann, A., Rillig, M.C., Solé, R.V., Maestre, F.T., 2020. Global ecosystem thresholds driven by aridity. Science 367, 787–790. https://doi.org/10.1126/science.aay5958.

Bloom, A.A., Bowman, K.W., Liu, J., Konings, A.G., Worden, J.R., Parazoo, N.C., Meyer, V., Reager, J.T., Worden, H.M., Jiang, Z., Quetin, G.R., Smallman, T.L., Exbrayat, J.-F., Yin, Y., Saatchi, S.S., Williams, M., Schimel, D.S., 2020. Lagged effects regulate the inter-annual variability of the tropical carbon balance. Biogeosciences 17, 6393–6422. https://doi.org/10.5194/bg-17-6393-2020.

Briceño-J, A.M., Rangel-Ch, J.O., Bogino, S.M., 2016. DE Cordia alliodora (Ruiz & Pav.) Oken EN COLOMBIA. Colomb. For. 19, 14.

Brienen, R.J.W., Schöngart, J., Zuidema, P.A., 2016. Tree rings in the tropics: insights into the ecology and climate sensitivity of tropical trees. In: Goldstein, G., Santiago, L.S. (Eds.), Tropical Tree Physiology. Springer International Publishing, Cham, pp. 439–461. https://doi.org/10.1007/978-3-319-27422-5_20.

Brodribb, T.J., Powers, J., Cochard, H., Choat, B., 2020. Hanging by a thread? Forests and drought. Science 368, 261–266. https://doi.org/10.1126/science.aat7631.

Bunn, A., Korpela, M., Biondi, F., Campelo, F., Mérian, P., Qeadan, F., Zang, C., Buras, A., Cecile, J., Mudelsee, M., Schulz, M., 2017. "dplR": Dendrochronology Program Library in R.

Butz, P., Hölscher, D., Cueva, E., Graefe, S., 2018. Tree water use patterns as influenced by phenology in a dry forest of southern ecuador. Front. Plant Sci. 9, 945. https://doi.org/10.3389/fpls.2018.00945.

Camarero, J.J., Manzanedo, R.D., Sanchez-Salguero, R., Navarro-Cerrillo, R.M., 2013. Growth response to climate and drought change along an aridity gradient in the southernmost Pinus nigra relict forests. Ann. For. Sci. 70, 769–780. https://doi.org/10.1007/s13595-013-0321-9.

Castello, A.C.D., de Souza Pereira, A.S., Messias, P.A., Scudeler, A.L., de Moura, Y.A., Koch, I., 2018. Two new species of *Aspidosperma* (Apocynaceae) from Northeast Brazil and a monograph of the species from Ceará State. Syst. Bot. 43, 1030–1045. https://doi.org/10.1600/036364418X697742.

Chazdon, R.L., Broadbent, E.N., Rozendaal, D.M.A., Bongers, F., Zambrano, A.M.A., Aide, T.M., Balvanera, P., Becknell, J.M., Boukili, V., Brancalion, P.H.S., Craven, D., Almeida-Cortez, J.S., Cabral, G.A.L., de Jong, B., Denslow, J.S., Dent, D.H., DeWalt, S.J., Dupuy, J.M., Durán, S.M., Espírito-Santo, M.M., Fandino, M.C., César, R.G., Hall, J.S., Hernández-Stefanoni, J.L., Jakovac, C.C., Junqueira, A.B., Kennard, D., Letcher, S.G., Lohbeck, M., Martínez-Ramos, M., Massoca, P., Meave, J. A., Mesquita, R., Mora, F., Muñoz, R., Muscarella, R., Nunes, Y.R.F., Ochoa-Gaona, S., Orihuela-Belmonte, E., Peña-Claros, M., Pérez-García, E.A., Piotto, D., Powers, J.S., Rodríguez-Velazquez, J., Romero-Pérez, I.E., Ruíz, J., Saldarriaga, J.G., Sanchez-Azofeifa, A., Schwartz, N.B., Steininger, M.K., Swenson, N.G., Uriarte, M., van Breugel, M., van der Wal, H., Veloso, M.D.M., Vester, H., Vieira, I.C.G., Bentos, T.V., Williamson, G.B., Poorter, L., 2016. Carbon sequestration potential of second-growth forest regeneration in the Latin American tropics. Sci. Adv. 2, e1501639 https://doi.org/10.1126/sciadv.1501639.

Chen, C., Park, T., Wang, X., Piao, S., Xu, B., Chaturvedi, R.K., Fuchs, R., Brovkin, V., Ciais, P., Fensholt, R., Tømmervik, H., Bala, G., Zhu, Z., Nemani, R.R., Myneni, R.B., 2019. China and India lead in greening of the world through land-use management. Nat. Sustain. 2, 122–129. https://doi.org/10.1038/s41893-019-0220-7.

Ciemer, C., Boers, N., Hirota, M., Kurths, J., Müller-Hansen, F., Oliveira, R.S., Winkelmann, R., 2019. Higher resilience to climatic disturbances in tropical vegetation exposed to more variable rainfall. Nat. Geosci. 12, 174–179. https://doi.org/10.1038/s41561-019-0312-z.

Correia Filho, W.L.F., De Oliveira-Júnior, J.F., De Barros Santiago, D., De Bodas Terassi, P.M., Teodoro, P.E., De Gois, G., Blanco, C.J.C., De Almeida Souza, P.H., da Silva Costa, M., Gomes, H.B., Dos Santos, P.J., 2019. Rainfall variability in the Brazilian northeast biomes and their interactions with meteorological systems and ENSO via CHELSA product. Big Earth Data 3, 315–337. https://doi.org/10.1080/20964471.2019.1692298.

Cybis, 2020. CooRecoder basics [WWW Document]. URL ⟨http://www.cybis.se/forfun/dendro/helpcoorecorder7/index.php⟩ (Accessed 2.22.20).

Espinosa, C.I., Camarero, J.J., Gusmán, A.A., 2018. Site-dependent growth responses to climate in two major tree species from tropical dry forests of southwest Ecuador. Dendrochronologia 52, 11–19. https://doi.org/10.1016/j.dendro.2018.09.004.

Estrada-Medina, H., Santiago, L.S., Graham, R.C., Allen, M.F., Jiménez-Osornio, J.J., 2013. Source water, phenology and growth of two tropical dry forest tree species growing on shallow karst soils. Trees 27, 1297–1307. https://doi.org/10.1007/s00468-013-0878-9.

FAO, 2014. World Reference Base for Soil Resources 2014: International Soil Classification System for Naming Soils and Creating Legends for Soil Maps. FAO, Rome.

Felsenstein, J., 1985. Phylogenies and the comparative method. Am. Nat. 125, 1–15. https://doi.org/10.1086/284325.

Fernandes, M.F., Cardoso, D., de Queiroz, L.P., 2020. An updated plant checklist of the Brazilian Caatinga seasonally dry forests and woodlands reveals high species richness and endemism. J. Arid Environ. 174, 104079 https://doi.org/10.1016/j.jaridenv.2019.104079.

Fernández Otárola, M., Sazima, M., Solferini, V.N., 2016. Stem and crown allometry in four congeneric species of dioecious tropical trees. Trees 30, 2041–2049. https://doi.org/10.1007/s00468-016-1431-4.

Fichtler, E., Worbes, M., 2012. Wood anatomical variables in tropical trees and their relation to site conditions and individual tree morphology. IAWA J. 33, 119–140. https://doi.org/10.1163/22941932-90000084.

Fontana, C., Pérez-de-Lis, G., Nabais, C., Lousada, J.L.P.C., Olmedo, G.M., Botosso, P.C., Oliveira, J.M., 2018. Climatic signal in growth-rings of Copaifera lucens: an endemic species of a Brazilian Atlantic forest hotspot, southeastern Brazil. Dendrochronologia 50, 23–32. https://doi.org/10.1016/j.dendro.2018.04.004.

Frank, Dorothea, Reichstein, M., Bahn, M., Thonicke, K., Frank, David, Mahecha, M.D., Smith, P., Velde, M., Vicca, S., Babst, F., Beer, C., Buchmann, N., Canadell, J.G., Ciais, P., Cramer, W., Ibrom, A., Miglietta, F., Poulter, B., Rammig, A., Seneviratne, S.I., Walz, A., Wattenbach, M., Zavala, M.A., Zscheischler, J., 2015. Effects of climate extremes on the terrestrial carbon cycle: concepts, processes and potential future impacts. Glob. Change Biol. 21, 2861–2880. https://doi.org/10.1111/gcb.12916.

Funceme, 2020. Postos pluviométricos. Fundação Cearense de Meteorologia e Recursos Hídricos - FUNCEME [WWW Document]. URL ⟨http://www.funceme.br/?page_id=2694⟩.

Gao, S., Liu, R., Zhou, T., Fang, W., Yi, C., Lu, R., Zhao, X., Luo, H., 2018. Dynamic responses of tree-ring growth to multiple dimensions of drought. Glob. Change Biol. 24, 5380–5390. https://doi.org/10.1111/gcb.14367.

Gärtner, H., Cherubini, P., Fonti, P., von Arx, G., Schneider, L., Nievergelt, D., Verstege, A., Bast, A., Schweingruber, F.H., Büntgen, U., 2015. A technical perspective in modern tree-ring research - how to overcome dendroecological and wood anatomical challenges. J. Vis. Exp. 1–10. https://doi.org/10.3791/52337.

Godoy-Veiga, M., Cintra, B.B.L., Stríkis, N.M., Cruz, F.W., Grohmann, C.H., Santos, M.S., Regev, L., Boaretto, E., Ceccantini, G., Locosselli, G.M., 2021. The value of climate responses of individual trees to detect areas of climate-change refugia, a tree-ring study in the Brazilian seasonally dry tropical forests. For. Ecol. Manag. 488, 118971 https://doi.org/10.1016/j.foreco.2021.118971.

Gradel, A., Ganbaatar, B., Nadaldorj, O., Dovdondemberel, B., Kusbach, A., 2017a. Climate-growth relationships and pointer year analysis of a Siberian larch (Larix sibirica Ledeb.) chronology from the Mongolian mountain forest steppe compared to white birch (Betula platyphylla Sukaczev). . Ecosyst. 4, 22. https://doi.org/10.1186/s40663-017-0110-2.

Gradel, A., Haensch, C., Ganbaatar, B., Dovdondemberel, B., Nadaldorj, O., Günther, B., 2017b. Response of white birch (Betula platyphylla Sukaczev) to temperature and precipitation in the mountain forest steppe and taiga of northern Mongolia. Dendrochronologia 41, 24–33. https://doi.org/10.1016/j.dendro.2016.03.005.

Granato-Souza, D., Adenesky-Filho, E., Esemann-Quadros, K., 2018. Dendrochronology and climatic signals in the wood of Nectandra oppositifolia from a dense rain forest in southern Brazil. J. . Res. https://doi.org/10.1007/s11676-018-0687-5.

Harris, I., Osborn, T.J., Jones, P., Lister, D., 2020. Version 4 of the CRU TS monthly high-resolution gridded multivariate climate dataset. Sci. Data 7, 109. https://doi.org/10.1038/s41597-020-0453-3.

Hogan, J.A., Nytch, C.J., Bithorn, J.E., Zimmerman, J.K., 2019. Proposing the solar wind-energy-flux hypothesis as a driver of interannual variation in tropical tree reproductive effort tropical tree reproduction (preprint). Plant Biol. https://doi.org/10.1101/606871.

Holmes, R.L., 1983. Computer-assisted quality control in tree-ring dating and measurement. Tree Ring Bull. 43, 69–78.

Hughes, M.K., Swetnam, T.W., Diaz, H.F. (Eds.), 2011. Dendroclimatology, Developments in Paleoenvironmental Research. Springer, Netherlands, Dordrecht.

Humphrey, V., 2021. Soil moisture–atmosphere feedback dominates land carbon uptake variability. Nature 592, 18. https://doi.org/10.1038/s41586-021-03325-5.

IPCC, C.C. 2014, 2014. Impacts, Adaptation, and Vulnerability. Part A: Global and Sectoral Aspects. Contribution of Working Group II to the Fifth Assessment Report of the Intergovernmental Panel on Climate Change [WWW Document]. URL ⟨http://www.ipcc.ch/report/ar5/wg2/⟩ (Accessed 4.17.17).

Jimenez, J.C., Marengo, J.A., Alves, L.M., Sulca, J.C., Takahashi, K., Ferrett, S., Collins, M., 2019. The role of ENSO flavours and TNA on recent droughts over Amazon forests and the Northeast Brazil region. Int. J. Climatol. https://doi.org/10.1002/joc.6453 (joc. 6453).

Kannenberg, S.A., Schwalm, C.R., Anderegg, W.R.L., 2020. Ghosts of the past: how drought legacy effects shape forest functioning and carbon cycling. Ecol. Lett. 23, 891–901. https://doi.org/10.1111/ele.13485.

Köppen, W., 1948. Climatologia. Fondo de Cultura Econòmica, México.

Land, A., Remmele, S., Schönbein, J., Küppers, M., Zimmermann, R., 2017. Climate-growth analysis using long-term daily-resolved station records with focus on the effect of heavy precipitation events. Dendrochronologia 45, 156–164. https://doi.org/10.1016/j.dendro.2017.08.005.

Le Quéré, C., Andrew, R.M., Friedlingstein, P., Sitch, S., Hauck, J., Pongratz, J., Pickers, P.A., Korsbakken, J.I., Peters, G.P., Canadell, J.G., Arneth, A., Arora, V.K., Barbero, L., Bastos, A., Bopp, L., Chevallier, F., Chini, L.P., Ciais, P., Doney, S.C., Gkritzalis, T., Goll, D.S., Harris, I., Haverd, V., Hoffman, F.M., Hoppema, M., Houghton, R.A., Hurtt, G., Ilyina, T., Jain, A.K., Johannessen, T., Jones, C.D., Kato, E., Keeling, R.F., Goldewijk, K.K., Landschützer, P., Lefèvre, N., Lienert, S., Liu, Z., Lombardozzi, D., Metzl, N., Munro, D.R., Nabel, J.E.M.S., Nakaoka, S., Neill, C., Olsen, A., Ono, T., Patra, P., Peregon, A., Peters, W., Peylin, P., Pfeil, B., Pierrot, D., Poulter, B., Rehder, G., Resplandy, L., Robertson, E., Rocher, M., Rödenbeck, C., Schuster, U., Schwinger, J., Séférian, R., Skjelvan, I., Steinhoff, T., Sutton, A., Tans, P.P., Tian, H., Tilbrook, B., Tubiello, F.N., van der Laan-Luijkx, I.T., van der Werf, G.R., Viovy, N., Walker, A.P., Wiltshire, A.J., Wright, R., Zaehle, S., Zheng, B., 2018. Global Carbon Budget 2018. Earth Syst. Sci. Data 10, 2141–2194. https://doi.org/10.5194/essd-10-2141-2018.

Lemos, J.R., Meguro, M., 2010. Florística e Fitogeografia da Vegetação Decidual da Estação Ecológica de Aiuaba, 8. Nordeste do Brasil, Ceará, p. 10.

Linscheid, N., Estupinan-Suarez, L.M., Brenning, A., Carvalhais, N., Cremer, F., Gans, F., Rammig, A., Reichstein, M., Sierra, C.A., Mahecha, M.D., 2020. Towards a global understanding of vegetation–climate dynamics at multiple timescales. Biogeosciences 17, 945–962. https://doi.org/10.5194/bg-17-945-2020.

Lisi, C.S., Pagotto, M.A., Anholetto, C.R., Nogueira, F.C., Santos, H.L., Costa, C.M., Menezes, Í.R.N., Roig Juñet, F.A., Tommasiello Filho, M., 2020. Dendroecological studies with Cedrela odorata L., Northeastern Brazil. In: Pompa-García, M., Camarero, J.J. (Eds.), Latin American Dendroecology. Springer International Publishing, Cham, pp. 37–59. https://doi.org/10.1007/978-3-030-36930-9_3.

Liu, L., Gudmundsson, L., Hauser, M., Qin, D., Li, S., Seneviratne, S.I., 2020. Soil moisture dominates dryness stress on ecosystem production globally. Nat. Commun. 11, 4892. https://doi.org/10.1038/s41467-020-18631-1.

Locosselli, G.M., Buckeridge, M.S., Moreira, M.Z., Ceccantini, G., 2013. A multi-proxy dendroecological analysis of two tropical species (Hymenaea spp., Leguminosae) growing in a vegetation mosaic. Trees 27, 25–36. https://doi.org/10.1007/s00468-012-0764-x.

Locosselli, G.M., Krottenthaler, S., Pitsch, P., Anhuf, D., Ceccantini, G., 2017. Age and growth rate of congeneric tree species (Hymenaea spp. - Leguminosae) inhabiting different tropical biomes. Erdkunde 71, 45–57. https://doi.org/10.3112/erdkunde.2017.01.03.

López, L., Rodríguez-Catón, M., Villalba, R., 2019. Convergence in growth responses of tropical trees to climate driven by water stress. Ecography 42, 1899–1912. https://doi.org/10.1111/ecog.04296.

López, L., Villalba, R., 2020. Climate-growth relationships for Aspidosperma tomentosum Mart. in South American tropical dry forests. Ann. For. Sci. 77, 96. https://doi.org/10.1007/s13595-020-01001-8.

Marengo, J.A., Alves, L.M., Alvala, R.C.S., Cunha, A.P., Brito, S., Moraes, O.L.L., 2017. Climatic characteristics of the 2010-2016 drought in the semiarid Northeast Brazil region. An. Acad. Bras. Ciênc. https://doi.org/10.1590/0001-3765201720170206.

Marengo, J.A., Liebmann, B., Grimm, A.M., Misra, V., Silva Dias, P.L., Cavalcanti, I.F.A., Carvalho, L.M.V., Berbery, E.H., Ambrizzi, T., Vera, C.S., Saulo, A.C., Nogues-Paegle, J., Zipser, E., Seth, A., Alves, L.M., 2012. Recent developments on the South American monsoon system. Int. J. Climatol. 32, 1–21. https://doi.org/10.1002/joc.2254.

Matos, M. de Q., Felfili, J.M., 2010. Florística, fitossociologia e diversidade da vegetação arbórea nas matas de galeria do Parque Nacional de Sete Cidades (PNSC), Piauí, Brasil. Acta Bot. Bras. 24, 483–496. https://doi.org/10.1590/S0102-33062010000200019.

Meko, D.M., Stahle, D.W., Griffin, D., Knight, T.A., 2011. Inferring precipitation-anomaly gradients from tree rings. Quat. Int. 235, 89–100. https://doi.org/10.1016/j.quaint.2010.09.006.

Moro, M.F., Macedo, M.B., Moura-Fé, M.M., de, Castro, A.S.F., Costa, R.C. da, 2015. Vegetação, unidades fitoecológicas e diversidade paisagística do estado do Ceará. Rodriguésia 66, 717–743. https://doi.org/10.1590/2175-7860201566305.

Moro, M.F., Nic Lughadha, E., de Araújo, F.S., Martins, F.R., 2016. A phytogeographical metaanalysis of the semiarid Caatinga Domain in Brazil. Bot. Rev. 82, 91–148. https://doi.org/10.1007/s12229-016-9164-z.

Nogueira Jr., F., de, C., Pagotto, M.A., Aragão, J.R.V., Roig, F.A., Ribeiro, A. de S., Lisi, C. S., 2019. The hydrological performance of Prosopis juliflora (Sw.) growth as an invasive alien tree species in the semiarid tropics of northeastern Brazil. Biol. Invasions. https://doi.org/10.1007/s10530-019-01994-y.

Nogueira Jr, F. de C., Pagotto, M.A., Roig, F.A., Lisi, C.S., Ribeiro, A. de S., 2017. Responses of tree-ring growth in Schinopsis brasiliensis to climate factors in the dry forests of northeastern Brazil. Trees. https://doi.org/10.1007/s00468-017-1642-3.

Relation of soils and geomorphic surfaces in the Brazilian Cerrado. In: Oliveira, P.S., Marquis, R.J. (Eds.), 2002. The Cerrados of Brazil. Columbia University Press, pp. 13–32. https://doi.org/10.7312/oliv12042-001.

Olson, D.M., Dinerstein, E., Wikramanayake, E.D., Burgess, N.D., Powell, G.V., Underwood, E.C., D'amico, J.A., Itoua, I., Strand, H.E., Morrison, J.C., et al., 2001. Terrestrial ecoregions of the world: a new map of life on earth a new global map of terrestrial ecoregions provides an innovative tool for conserving biodiversity. BioScience 51, 933–938.

Orvis, K.H., Grissino-Mayer, H.D., 2002. Standardizing the reporting of abrasive papers used to surface tree-ring samples. Tree Ring Res. 47–50.

Pace, M.R., Lohmann, L.G., Olmstead, R.G., Angyalossy, V., 2015. Wood anatomy of major Bignoniaceae clades. Plant Syst. Evol. 301, 967–995. https://doi.org/10.1007/s00606-014-1129-2.

Pennington, R.T., Lehmann, C.E.R., Rowland, L.M., 2018. Tropical savannas and dry forests. Curr. Biol. 28, R541–R545. https://doi.org/10.1016/j.cub.2018.03.014.

Pereira, G., de, A., Barbosa, A.C.M.C., Torbenson, M.C.A., Stahle, D.W., Granato-Souza, D., Santos, R.M.D., Barbosa, J.P.D., 2018. The climate response of *Cedrela fissilis* annual ring width in the Rio São Francisco Basin, Brazil. Tree Ring Res. 74, 162–171. https://doi.org/10.3959/1536-1098-74.2.162.

Pereira, M.P.S., Justino, F., Malhado, A.C.M., Barbosa, H., Marengo, J., 2014. The influence of oceanic basins on drought and ecosystem dynamics in Northeast Brazil. Environ. Res. Lett. 9, 124013 https://doi.org/10.1088/1748-9326/9/12/124013.

Pereira, M.P.S., Mendes, K.R., Justino, F., Couto, F., da Silva, A.S., da Silva, D.F., Malhado, A.C.M., 2020. Brazilian dry forest (Caatinga) response to multiple ENSO: the role of Atlantic and Pacific Ocean. Sci. Total Environ. 705, 135717 https://doi.org/10.1016/j.scitotenv.2019.135717.

Piao, S., Wang, X., Park, T., Chen, C., Lian, X., He, Y., Bjerke, J.W., Chen, A., Ciais, P., Tømmervik, H., Nemani, R.R., Myneni, R.B., 2020a. Characteristics, drivers and feedbacks of global greening. Nat. Rev. Earth Environ. 1, 14–27. https://doi.org/10.1038/s43017-019-0001-x.

Piao, S., Wang, X., Wang, K., Li, X., Bastos, A., Canadell, J.G., Ciais, P., Friedlingstein, P., Sitch, S., 2020b. Interannual variation of terrestrial carbon cycle: issues and perspectives. Glob. Change Biol. 26, 300–318. https://doi.org/10.1111/gcb.14884.

Pompa-García, M., Camarero, J.J. (Eds.), 2020. Latin American Dendroecology: Combining Tree-Ring Sciences and Ecology in a Megadiverse Territory. Springer International Publishing, Cham. https://doi.org/10.1007/978-3-030-36930-9.

Poulter, B., Frank, D., Ciais, P., Myneni, R.B., Andela, N., Bi, J., Broquet, G., Canadell, J. G., Chevallier, F., Liu, Y.Y., Running, S.W., Sitch, S., van der Werf, G.R., 2014. Contribution of semi-arid ecosystems to interannual variability of the global carbon cycle. Nature 509, 600–603. https://doi.org/10.1038/nature13376.

Queiroz, L.P., Cardoso, D., Fernandes, M.F., Moro, M.F., 2017. Diversity and evolution of flowering plants of the Caatinga Domain. In: Silva, J.M.C. da, Leal, I.R., Tabarelli, M. (Eds.), Caatinga. Springer International Publishing, Cham, pp. 23–63. https://doi.org/10.1007/978-3-319-68339-3_2.

R Core Team, 2015. R: A language and environment for statistical computing [WWW Document]. R Found. Stat. Comput. URL ⟨https://www.r-project.org/⟩ (Accessed 4.17.17).

Reynolds, R.W., Smith, T.M., 1994. Improved global sea surface temperature analyses using optimum interpolation. J. Clim. 7, 929–948. https://doi.org/10.1175/1520-0442(1994)007<0929:IGSSTA>2.0.CO;2.

Santos, H.G., dos, Pares, J.G., Carvalho Júnior, W., Fontana, A., Dart, R.O., Martin, A.L. S., Áglio, M.L.D., Oliveira, A.P., Souza, J.S., 2011. O Novo Mapa de Solos do Brasil: Legenda Atualizada, 1a. ed. Embrapa Solos, Rio de Janeiro.

Santos, H.G., Jacomine, P.K.T., Anjos, L.H.C., Oliveiva, V.A., Lumbreras, J.F., Coelho, M. R., Almeida, J.A., Araújo Filho, J.A., Oliveira, J.B., Cunha, T.J.F., 2018. Sistema Brasileiro de Classificação de Solos. 5a edição revista e ampliada. ed. Embrapa Solos, Brasília, DF.

Schöngart, J., Bräuning, A., Barbosa, A.C.M.C., Lisi, C.S., de Oliveira, J.M., 2017. Dendroecological studies in the neotropics: history, status and future challenges. In: Amoroso, M.M., Daniels, L.D., Baker, P.J., Camarero, J.J. (Eds.), Dendroecology. Springer International Publishing, Cham, pp. 35–73. https://doi.org/10.1007/978-3-319-61669-8_3.

Schulman, E., 1956. Dendroclimatic changes in semiarid America. University of Arizona Press, Tucson, Arizona, USA.

Schweingruberl, F.H., Aellen-Rum, K., Weber, U., Wehrli, U., 1990. Rhythmic growth fluctuations in forest trees of Central Europe and the Front Range in Colorado. Trees 4, 99–106.

Silva, J.M.C., da, Barbosa, L.C.F., Leal, I.R., Tabarelli, M., 2017. The Caatinga: understanding the challenges. In: Silva, J.M.C. da, Leal, I.R., Tabarelli, M. (Eds.), Caatinga. Springer International Publishing, Cham, pp. 3–19. https://doi.org/10.1007/978-3-319-68339-3_1.

Silveira, A.P., Menezes, B.S. de, Loiola, M.I.B., Lima-Verde, L.W., Zanina, D.N. e, Carvalho, E.C.D. de, Souza, B.C. de, Costa, R.C. da, Mantovani, W., Menezes, M.O.T. de, Flores, L.M.A., Nogueira, F.C.B., Matias, L.Q., Barbosa, L.S., Gomes, F.M., Cordeiro, L.S., Sampaio, V. da S., Batista, M.E.P., Soares Neto, R.L., Silva, M.A.P. da, Campos, N.B., Oliveira, A.A. de, Araujo, F.S. de, 2020. Flora and annual distribution of flowers and fruits in the Ubajara National Park, Ceará, Brazil. Floresta Ambient. 27, e20190058 https://doi.org/10.1590/2179-8087.005819.

Sitch, S., Smith, B., Prentice, I.C., Arneth, A., Bondeau, A., Cramer, W., Kaplan, J.O., Levis, S., Lucht, W., Sykes, M.T., Thonicke, K., Venevsky, S., 2003. Evaluation of ecosystem dynamics, plant geography and terrestrial carbon cycling in the LPJ dynamic global vegetation model. Glob. Change Biol. 9, 161–185. https://doi.org/10.1046/j.1365-2486.2003.00569.x.

Soil Survey Staff, 2014. Keys to Soil Taxonomy, 12a. ed. USDA-Natural Resources Conservation Service, Washington, DC.

Speer, J.H., 2010. Fundamentals of Tree-Ring Research. University of Arizona Press, Tucson.

Stan, K., Sanchez-Azofeifa, A., 2019. Tropical dry forest diversity, climatic response, and resilience in a changing climate. Forests 10, 443. https://doi.org/10.3390/f10050443.

Trouet, V., Van Oldenborgh, G.J., 2013. KNMI climate explorer: a web-based research tool for high-resolution paleoclimatology. Tree Ring Res. 69, 3–13. https://doi.org/10.3959/1536-1098-69.1.3.

Utida, G., Cruz, F.W., Etourneau, J., Bouloubassi, I., Schefuß, E., Vuille, M., Novello, V.F., Prado, L.F., Sifeddine, A., Klein, V., Zular, A., Viana, J.C.C., Turcq, B., 2019. Tropical South Atlantic influence on Northeastern Brazil precipitation and ITCZ displacement

during the past 2300 years. Sci. Rep. 9, 1698. https://doi.org/10.1038/s41598-018-38003-6.
van der Maaten-Theunissen, M., van der Maaten, E., Bouriaud, O., 2015. pointRes: an R package to analyze pointer years and components of resilience. Dendrochronologia 35, 34–38. https://doi.org/10.1016/j.dendro.2015.05.006.
Walter, H., Lieth, H., 1960. Klimadiagram-Weltatlas. Gustav Fisch. Verl. 40.
Wang, J., Zeng, N., Wang, M., 2016. Interannual variability of the atmospheric CO2 growth rate: roles of precipitation and temperature. Biogeosciences 13, 2339–2352. https://doi.org/10.5194/bg-13-2339-2016.
Williams, B.K., Brown, E.D., 2019. Sampling and analysis frameworks for inference in ecology. Methods Ecol. Evol. 10, 1832–1842. https://doi.org/10.1111/2041-210X.13279.
Worbes, M., 2010. Wood anatomy and tree-ring structure and their importance for tropical dendrochronology. In: Junk, W.J., Piedade, M.T.F., Wittmann, F., Schöngart, J., Parolin, P. (Eds.), Amazonian Floodplain Forests. Springer, Netherlands, Dordrecht, pp. 329–346. https://doi.org/10.1007/978-90-481-8725-6_17.
Wu, H., Zou, Y., Alves, L.M., Macau, E.E.N., Sampaio, G., Marengo, J.A., 2020. Uncovering episodic influence of oceans on extreme drought events in Northeast Brazil by ordinal partition network approaches. Chaos Interdiscip. J. Nonlinear Sci. 30, 053104 https://doi.org/10.1063/5.0004348.
Xu, L., Saatchi, S.S., Yang, Y., Yu, Y., Pongratz, J., Bloom, A.A., Bowman, K., Worden, J., Liu, J., Yin, Y., Domke, G., McRoberts, R.E., Woodall, C., Nabuurs, G.-J., de-Miguel, S., Keller, M., Harris, N., Maxwell, S., Schimel, D., 2021. Changes in global terrestrial live biomass over the 21st century. Sci. Adv. 7, eabe9829 https://doi.org/10.1126/sciadv.abe9829.
Zang, C., Biondi, F., 2015. treeclim: an R package for the numerical calibration of proxy-climate relationships. Ecography 38, 431–436. https://doi.org/10.1111/ecog.01335.
Zhang, A., Jia, G., 2020. ENSO-driven reverse coupling in interannual variability of pantropical water availability and global atmospheric CO $_2$ growth rate. Environ. Res. Lett. 15, 034006 https://doi.org/10.1088/1748-9326/ab66cc.
Zhao, L., Dai, A., Dong, B., 2018. Changes in global vegetation activity and its driving factors during 1982–2013. Agric. For. Meteorol. 249, 198–209. https://doi.org/10.1016/j.agrformet.2017.11.013.
Zuidema, P.A., Baker, P.J., Groenendijk, P., Schippers, P., van der Sleen, P., Vlam, M., Sterck, F., 2013. Tropical forests and global change: filling knowledge gaps. Trends Plant Sci. 18, 413–419. https://doi.org/10.1016/j.tplants.2013.05.006.
Zuidema, P.A., Frank, D., 2015. Forests: tree rings track climate trade-offs. Nature 523, 531–531.